Neocortical Neuronal Morphology in the Siberian Tiger (*Panthera tigris altaica*) and the Clouded Leopard (*Neofelis nebulosa*)

Cameron B. Johnson,[1] Matthew Schall,[1] Mackenzie E. Tennison,[1] Madeleine E. Garcia,[1] Noah B. Shea-Shumsky,[1] Mary Ann Raghanti,[2] Albert H. Lewandowski,[3] Mads F. Bertelsen,[4] Leona C. Waller,[1] Timothy Walsh,[5] John F. Roberts,[6] Patrick R. Hof,[7] Chet C. Sherwood,[8] Paul R. Manger,[9] and Bob Jacobs[1]*

[1]Laboratory of Quantitative Neuromorphology, Neuroscience Program, Colorado College, Colorado Springs, Colorado 80903
[2]Department of Anthropology and School of Biomedical Sciences, Kent State University, Kent, Ohio 44242
[3]Cleveland Metroparks Zoo, Cleveland, Ohio 44109
[4]Center for Zoo and Wild Animal Health, Copenhagen Zoo, 2000 Fredericksberg, Denmark
[5]Smithsonian National Zoological Park, Washington, DC 20008
[6]Thompson Bishop Sparks State Diagnostic Laboratory, Alabama Department of Agriculture and Industries, Auburn, Alabama 36849
[7]Fishberg Department of Neuroscience and Friedman Brain Institute, Icahn School of Medicine at Mount Sinai, New York, New York 10029
[8]Department of Anthropology, The George Washington University, Washington, DC 20052
[9]School of Anatomical Sciences, Faculty of Health Sciences, University of the Witwatersrand, Johannesburg, 2000, South Africa

ABSTRACT

Despite extensive investigations of the neocortex in the domestic cat, little is known about neuronal morphology in larger felids. To this end, the present study characterized and quantified the somatodendritic morphology of neocortical neurons in prefrontal, motor, and visual cortices of the Siberian tiger (*Panthera tigris altaica*) and clouded leopard (*Neofelis nebulosa*). After neurons were stained with a modified Golgi technique ($N = 194$), dendritic branching and spine distributions were analyzed using computer-assisted morphometry. Qualitatively, aspiny and spiny neurons in both species appeared morphologically similar to those observed in the domestic cat. Although the morphology of spiny neurons was diverse, with the presence of extraverted, inverted, horizontal, and multiapical pyramidal neurons, the most common variant was the typical pyramidal neuron. Gigantopyramidal neurons in the motor cortex were extremely large, confirming the observation of Brodmann ([1909] *Vergleichende Lokalisationlehre der Grosshirnrinde in ihren Prinzipien dargestellt auf Grund des Zellenbaues*. Leipzig, Germany: J.A. Barth), who found large somata for these neurons in carnivores in general, and felids in particular. Quantitatively, a MARSplines analysis of dendritic measures differentiated typical pyramidal neurons between the Siberian tiger and the clouded leopard with 93% accuracy. In general, the dendrites of typical pyramidal neurons were more complex in the tiger than in the leopards. Moreover, dendritic measures in tiger pyramidal neurons were disproportionally large relative to body/brain size insofar as they were nearly as extensive as those observed in much larger mammals (e.g., African elephant). Comparison of neuronal morphology in a more diverse collection of larger felids may elucidate the comparative context for the relatively large size of the pyramidal neurons observed in the present study. J. Comp. Neurol. 000:000–000, 2016.

INDEXING TERMS: dendrite; morphometry; Golgi method; brain evolution; neocortex

Grant sponsor: The James S. McDonnell Foundation; Grant numbers: 22002078 (to P.R.H. and C.C.S.) and 220020293 (to C.C.S.); Grant sponsor: South African National Research Foundation (to P.R.M.).

*CORRESPONDENCE TO: Bob Jacobs, Laboratory of Quantitative Neuromorphology, Neuroscience Program, Colorado College, 14 E. Cache La Poudre, Colorado Springs, CO 80903. E-mail: BJacobs@ColoradoCollege.edu

Received March 25, 2016; Revised April 18, 2016;
Accepted April 19, 2016.
DOI 10.1002/cne.24022
Published online Month 00, 2016 in Wiley Online Library (wileyonlinelibrary.com)

Felid neocortex research has historically focused on the domestic cat (*Felis catus*), which provided the source material for some of the first drawings of cortical neurons (Ramón y Cajal, 1911). Domestic cats were also the focus for many of the electrophysiological investigations of visual cortex in the latter half of the 20th century (Hubel and Wiesel, 1959, 1962; Anderson et al., 1988; Gilbert and Wiesel, 1989). More recent research on domestic cat neocortex has addressed topics such as morphomolecular markers (Hof and Sherwood, 2005; Van der Gucht et al., 2005; Mellott et al., 2010), cortical connectivity (Scannell et al., 1995; Thomson and Bannister, 2003; Higo et al., 2007), and neuronal morphometry (Matsubara et al., 1996; Elston, 2002). Despite such extensive exploration of the domestic cat neocortex, nondomestic feliforms have received little attention in neuroscience research (Manger et al., 2008), presumably for practical reasons. Recently, however, studies of neuronal morphology across a variety of previously unexplored large-brained mammals in both cerebellar (Jacobs et al., 2014) and cerebral cortex (Jacobs et al., 2011, 2015a,b; Butti et al., 2015) have revealed not only similarities but also some striking differences across species. To characterize further neuronal diversity across mammalian evolution, the present investigation extends existing knowledge of felid neocortex by examining the neocortical neuronal morphology of the Siberian tiger (*Panthera tigris altaica*) and the clouded leopard (*Neofelis nebulosa*).

Both the Siberian tiger and the clouded leopard belong to the Order Carnivora. Within Carnivora, the family Felidae originated during the late Miocene period, approximately 11 million years ago (Johnson et al., 2006). Within Felidae, mitochondrial and nuclear genomic analyses indicate that the clouded leopard and the genus *Panthera*, to which the Siberian tiger belongs, form a monophyletic group, suggesting that these species are relatively closely related (Yu and Zhang, 2005; Johnson et al., 2006). The Siberian tiger, which exhibits individualized home ranges in northeast Asia (Luo et al., 2004; Sun et al., 2005; Goodrich et al., 2010), is the largest extant felid, possessing the greatest average body weight (males: ~180–258 kg; females: ~100–160 kg) and skull size (Mazák, 1981) of any tiger. Brain weight for this species averages ~280 g, 4-fold greater than the ~70 g brain of the clouded leopard (Gittleman, 1986) and 9.3-fold greater than the ~30 g brain of the domestic cat. By comparison, the clouded leopard is an elusive, agile, largely arboreal, medium-sized cat (~11–23 kg body mass) native to mainland Southeast Asia and Indonesia (Hemmer, 1968; Nowell and Jackson, 1996; Buckley-Beason et al., 2006), although recent studies suggest that Indonesian clouded leopards are a separate species (*Neofelis diardi*; Kitchener et al., 2006; Wilting et al., 2007).

Although Siberian tiger and clouded leopard cerebral cortex has not been examined previously, research on the domestic cat and other felids suggests that neocortical anatomy in the present species should appear similar to that of primates and rodents in terms of laminar and columnar organization (Lund et al., 1979; Peters and Kara, 1985, 1987; Peters and Yilmaz, 1993; Mountcastle, 1997; Innocenti and Vercelli, 2010; DeFelipe, 2011). These architectural similarities appear to extend to synaptic connectivity (Thomson et al., 2002; Thomson and Bannister, 2003) and to qualitative aspects of neuronal morphology. The feline cortex is dominated by vertically oriented pyramidal neurons that become progressively larger in deeper cortical layers, with conspicuous gigantopyramidal neurons in layer V of primary motor cortex (Lewis, 1878; Phillips, 1956; Hassler and Muhs-Clement, 1964). In addition, a variety of nonpyramidal neurons (e.g., bitufted, bipolar, chandelier, stellate neurons) are found throughout the cortex, particularly in layer IV of primary sensory regions (O'Leary, 1941; Winer, 1984a,b,c, 1985; De Carlos et al., 1985; Vercelli and Innocenti, 1993). Quantitatively, much less is known about neocortical neuronal morphology in felids, although Sholl's (1953) initial analyses indicate differences in dendritic extent between neurons in motor and visual cortices.

To explore felid quantitative neuromorphology in more detail, the present study examined three cortical regions (prefrontal, primary motor, and primary visual) in the Siberian tiger and clouded leopard. The present data provide the first relatively comprehensive documentation of cortical neuromorphology in these felids, facilitating comparison with other species examined with the same methodology (e.g., elephant, giraffe, humpback whale). Moreover, we hypothesized that, insofar as increased mammalian brain size is accompanied by larger neurons (Kaas, 2000), Siberian tiger neurons would be larger than clouded leopard neurons for the majority of dependent measures, particularly volume and dendritic length. Finally, in accordance with previous research in elephants (Jacobs et al., 2011) and primates (Elston et al., 2001; Jacobs et al., 2001), we expected that pyramidal neurons in the prefrontal cortex would have more complex dendritic arbors (i.e., greater dendritic length and higher spine counts) than pyramidal neurons in visual or motor cortices—although the ability to test this hypothesis fully is constrained by the small number of pyramidal neurons traced in each region.

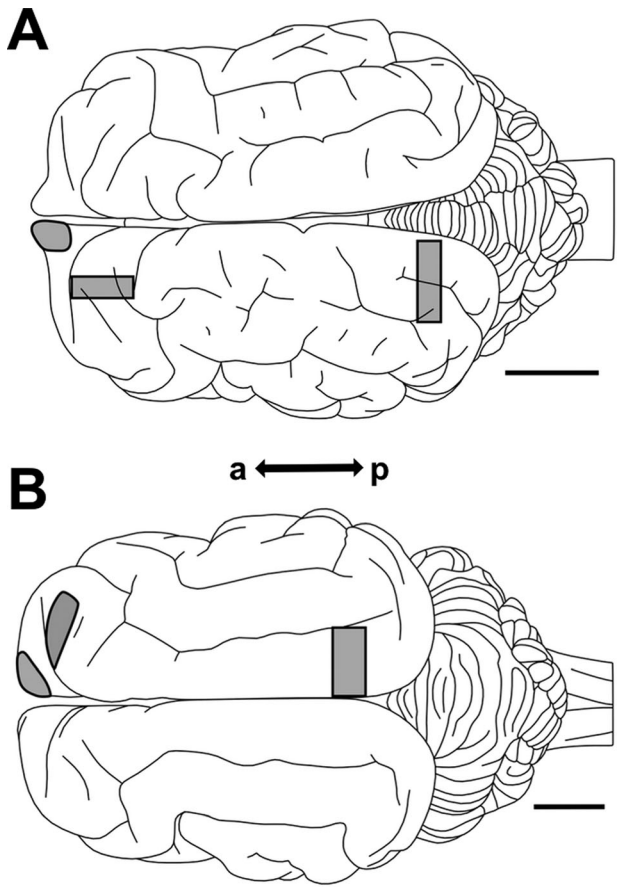

Figure 1. Dorsal view of the Siberian tiger (**A**) and clouded leopard (**B**) brains. Highlighted are the relative positions of cortical tissue sections used in the present study from anterior (a) to posterior (p): prefrontal cortex, primary motor cortex, primary visual cortex. Scale bar = 2 cm in A; 1 cm in B.

MATERIALS AND METHODS

Specimens

Because the animals in the present study were included in a comparative study on cerebellar neurons, specimen demographics are identical (Jacobs et al., 2014). The present study was approved by the Colorado College Institutional Review Board (#011311-1) and the University of the Witwatersrand Animal Ethics Committee (2008/36/1).

Siberian tiger

Cortical tissue from a 12-year-old female Siberian tiger (*Panthera tigris altaica*; ST) from the Copenhagen Zoo in Denmark was obtained following euthanasia. In situ perfusion–fixation (autolysis time < 30 minutes; by Mads F. Bertelsen) involved perfusing the head via the carotid artery with cold saline followed by 4% paraformaldehyde in 0.1 M phosphate buffer; following removal of the brain, tissue was placed in cold fixative and stored in 4% paraformaldehyde in 0.1 M phosphate buffer for 24 hours, after which the brain was stored in 0.1% sodium azide in 0.1 M phosphate-buffered saline at 4°C. Brain mass was 258 g. Prior to Golgi staining, tissue blocks containing prefrontal, motor, and visual cortices were stored in 0.1% sodium azide in 0.1 M phosphate buffer saline at 4°C for 6 months.

Clouded leopard

Tissue from two clouded leopard (*Neofelis nebulosa*; CL) brains was obtained following euthanasia: a 20-year-old female (CL1) from the Smithsonian National Zoological Park in Washington, DC, and a 28-year-old female (CL2) from the Cleveland Metroparks Zoo in Cleveland, OH (autolysis time < 30 minutes for both specimens). The brains were immersion-fixed in 10% formalin for 10 (CL1) and 34 days (CL2). Brain masses were 82 g (CL1) and 73 g (CL2). Prior to Golgi staining, tissue blocks from prefrontal, motor, and visual cortices were stored in 0.1% sodium azide in 0.1 M phosphate-buffered saline at 4°C for 5 months (CL1) and 3 years (CL2).

Tissue selection and preparation

Tissue blocks (3–5 mm thick) were removed from three regions of the left hemisphere in the Siberian tiger: 1) the dorsomedial aspect of the frontopolar cortex; 2) the primary motor cortex, located immediately posterior to the frontal pole and 1–2 cm lateral to the longitudinal fissure; and 3) the primary visual cortex, located along the dorsal posterior aspect of the lateral gyrus and 1–2 cm lateral to the longitudinal fissure (Fig. 1A). Homologous tissue blocks were also removed from the clouded leopard brains (Fig. 1B). Tissue was coded to prevent experimenter bias, stained with a modified rapid Golgi technique (Scheibel and Scheibel, 1978b), and sectioned serially at 120 μm with a Vibratome (Leica VT1000S, Leica Microsystems, Wetzlar, Germany). Adjacent sections (40 μm thick) of selected tissue were stained with 0.5% cresyl violet for cytoarchitectural comparisons (Fig. 2). Laminar and cortical thickness measures were determined by averaging measures of 10 different sampling locations for each region of interest (Table 1).

Neuron selection and quantification

Traced neurons conformed to established selection criteria (Anderson et al., 2009; Jacobs et al., 2011, 2015a,b), with an isolated soma near the center of the 120-μm section and relatively well impregnated, unobscured, and complete (i.e., nontruncated) dendritic projections. To provide a comprehensive morphological analysis, neurons were selected to encompass representative typologies in each species. Neurons were

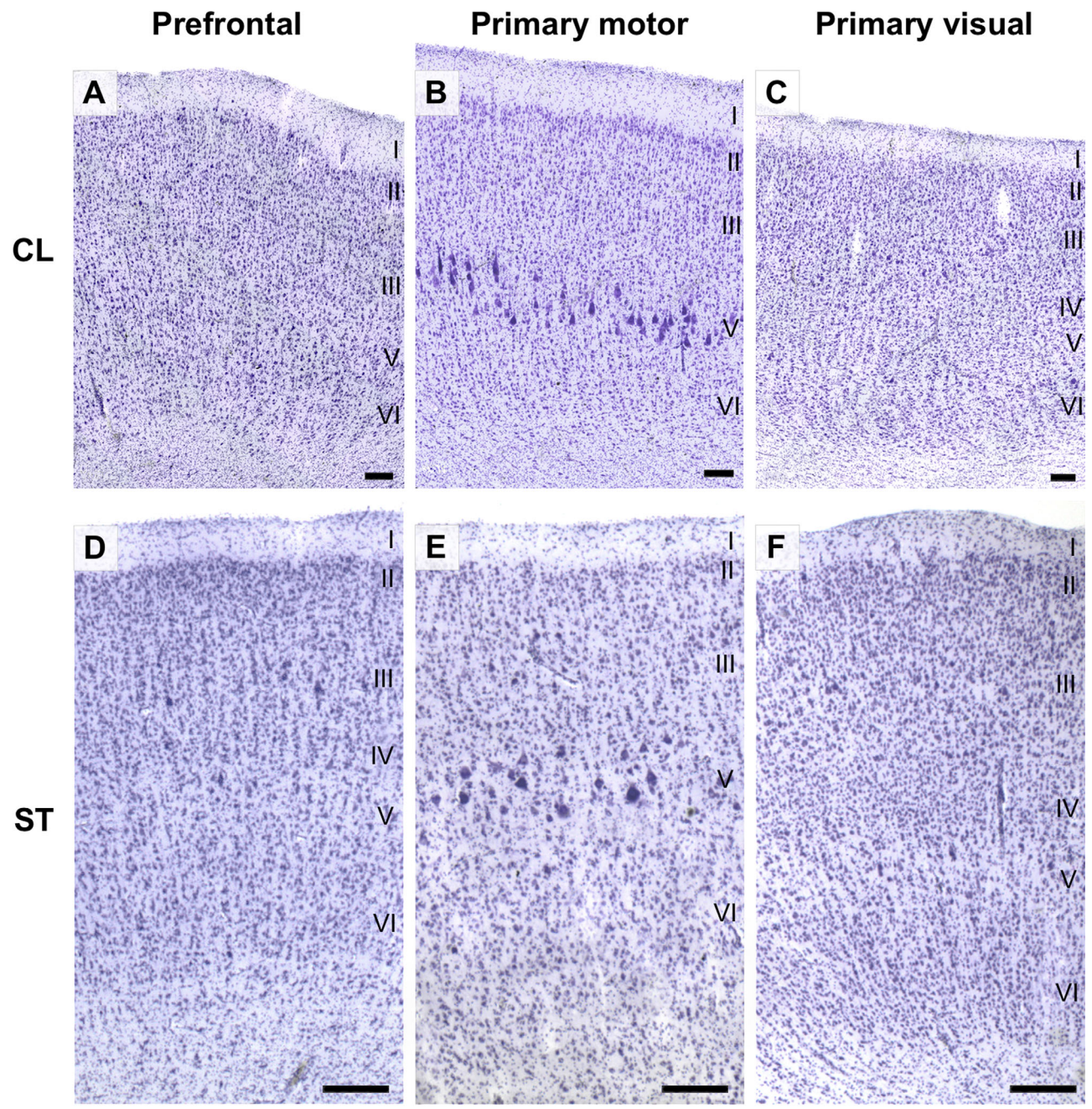

Figure 2. Photomicrographs of Nissl-stained tissue in the clouded leopard (CL) and Siberian tiger (ST): prefrontal (**A,D**), primary motor (**B,E**), and primary visual (**C,F**) cortices. Layers are labeled with Roman numerals. Layer IV is absent in Siberian tiger prefrontal (**D**) and primary motor (**E**) cortices, and in clouded leopard primary motor (**B**) cortex. Note also the presence of alternating minicolumns in layer VI of clouded leopard visual cortex (**C**). Gigantopyramidal neuron somata are readily evident in layer V of the primary motor cortex in both species (**B,E**). Scale bar = 100 μm in **A–C**; 250 μm in **D–F**. [Color figure can be viewed in the online issue, which is available at wileyonlinelibrary.com.]

quantified under a planachromatic 60× oil objective along x-, y-, and z-coordinates using a Neurolucida system (MBF Bioscience, Williston, VT; RRID: nif-0000-10294), interfaced with an Olympus BH-2 microscope equipped with a Ludl XY motorized stage (Ludl Electronics, Hawthorne, NY) and a Heidenhain z-axis encoder (Schaumburg, IL). A MicroFire Digital CCD 2-Megapixel camera (Optronics, Goleta, CA) mounted on a trinocular head (model 1-L0229, Olympus, Center Valley, PA) displayed images on a 1,920 × 1,200 resolution Dell E248WFP 24-inch LCD monitor. Somata were first traced at their widest point in the two-dimensional plane to provide an estimate of cross-sectional area. Dendrites were then traced somatofugally in their

TABLE 1.

Laminar and Cortical Thickness (μm) of Prefrontal, Primary Motor, and Primary Visual Cortices for Siberian Tiger (ST) and Clouded Leopard (CL)[1]

	Prefrontal cortex		Primary motor cortex		Primary visual cortex	
	ST	CL	ST	CL	ST	CL
Layer I	356 ± 48	208 ± 18	346 ± 32	187 ± 18	233 ± 20	136 ± 18
Layer II	179 ± 20	141 ± 6	160 ± 16	172 ± 21	134 ± 14	145 ± 13
Layer III	791 ± 167	562 ± 77	824 ± 44	510 ± 57	371 ± 68	545 ± 83
Layer IV	–	214 ± 25	–	–	416 ± 68	237 ± 19
Layer V	485 ± 55	310 ± 99	371 ± 40	449 ± 15	405 ± 41	317 ± 52
Layer VI	514 ± 76	533 ± 127	538 ± 81	581 ± 98	469 ± 56	517 ± 78
Total	2,325 ± 220	1,962 ± 216	2,239 ± 228	1,898 ± 45	2,018 ± 128	1,897 ± 45

[1]Values represent mean ± SD for 10 sampling locations in each region of interest.

entirety while accounting for dendritic diameter and quantity of spines. Dendritic arbors were not traced into neighboring sections; broken ends and indefinite terminations were labeled as incomplete endings. Neurons with sectioned segments were not differentially analyzed because elimination of such tracings would have biased the sample toward smaller neurons (Schadé and Caveness, 1968; Uylings et al., 1986). When present, axons were also traced, although they typically were not visible after a short distance.

Intra-rater reliability was established by having one investigator (L.W.) trace the same soma, dendritic segment, and spines 10 times. The coefficients of variation for soma size (5.2%), total dendritic length (TDL; 0.9%), and dendritic spine number (DSN; 1.3%) revealed minimal variation in tracings. Furthermore, a split plot design ($\alpha = 0.05$) indicated no significant difference between the first and last five tracings of the dataset. Inter-rater reliability was established by comparing 10 tracings of the same dendritic system between L.W. and the primary investigator (B.J.). Interclass correlation averages for soma size (0.99), TDL (0.96), and DSN (0.98) were not significantly different between investigators (analysis of variance [ANOVA] $\alpha = 0.05$). Additionally, the primary investigator re-examined all completed tracings under the microscope to ensure accuracy.

Neuron descriptions and dependent dendritic and spine measures

Descriptively, neurons were classified according to somatodendritic criteria (Ferrer et al., 1986a,b; Jacobs et al., 2011, 2015a,b) by considering factors such as soma size and shape, presence of spines, laminar location, and general morphology. Quantitatively, a centrifugal nomenclature was used to characterize branches extending from the soma as first-order segments, which bifurcate into second- and then third-order segments, and so on (Bok, 1959; Uylings et al., 1986). In addition to quantifying soma size (i.e., surface area [μm^2]) and depth from the pial surface (μm), we examined six other measures that have been analyzed in previous studies (Jacobs et al., 2011, 2015a,b): dendritic volume (Vol [μm^3]: the total volume of all dendrites); total dendritic length (TDL [μm]: the summed length of all dendritic segments); mean segment length (MSL [μm]: the average length of each dendritic segment); dendritic segment count (DSC: the number of dendritic segments); dendritic spine number (DSN: the total number of spines on dendritic segments); and dendritic spine density (DSD: the average number of spines per μm of dendritic length). Dendritic branching patterns were also analyzed using a Sholl analysis (Sholl, 1953), which quantified dendritic intersections at 20-μm intervals radiating somatofugally. All descriptive measures are presented as mean ± standard deviation (SD) unless noted otherwise.

Statistical analysis of species differences

Of traced neurons ($N = 194$), 72 were obtained from the Siberian tiger and 122 were obtained from the clouded leopards (CL1, 64; CL2, 58). Neurons were traced in prefrontal ($n = 61$; ST, 23; CL1, 20; CL2, 18), primary motor ($n = 68$; ST, 24; CL1, 22; CL2, 22), and primary visual cortices ($n = 65$; ST, 25; CL1, 22; CL2, 18). Only the numerically dominant pyramidal neurons ($n = 105$) were used for inferential analysis. By choosing a single homogeneous neuron type, we decreased artifactual variability that would result from inclusion of multiple neuron types. The examination of the dendritic characteristics of just three brains belonging to two species (ST, $n = 34$ pyramidal neurons; CL1, $n = 36$ pyramidal neurons; CL2, $n = 35$ pyramidal neurons) posed statistical challenges, as detailed in Jacobs et al. (2014). Insofar as accurate differentiation of species may require combinations of multiple dendritic measures, a more comprehensive analysis was necessary. We therefore examined species differences in dependent

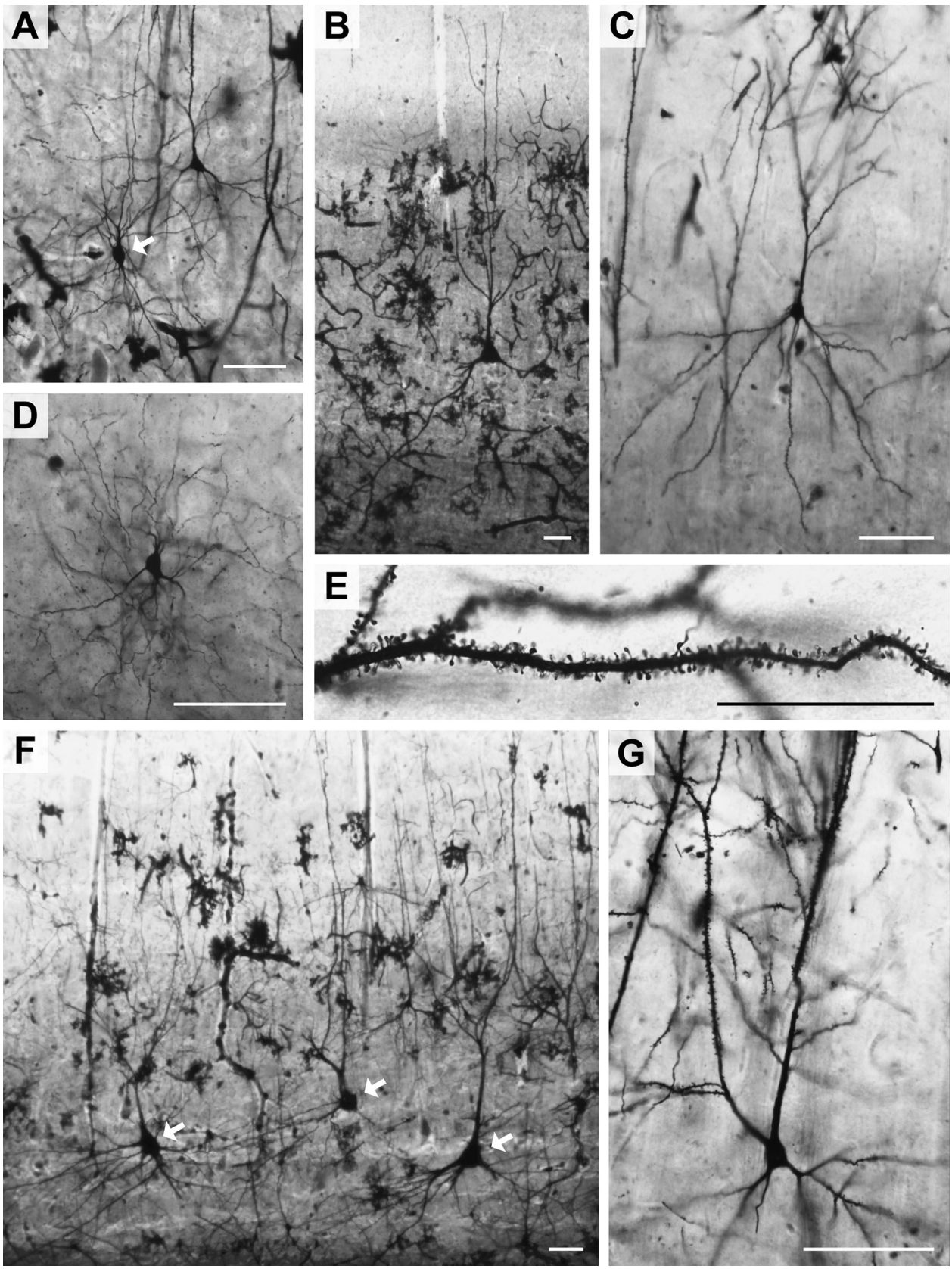

Figure 3. Photomicrographs of Golgi-stained neurons in primary motor (**A–C,F,G**) and prefrontal (**D,E**) cortices of the Siberian tiger: aspiny (**A**, arrow), gigantopyramidal (**B,F,** arrows), typical pyramidal (**C**), neurogliaform (**D**), and extraverted pyramidal (**E,G**) neurons. Scale bar = 100 μm in **A–D,F,G**; 50 μm in **E**.

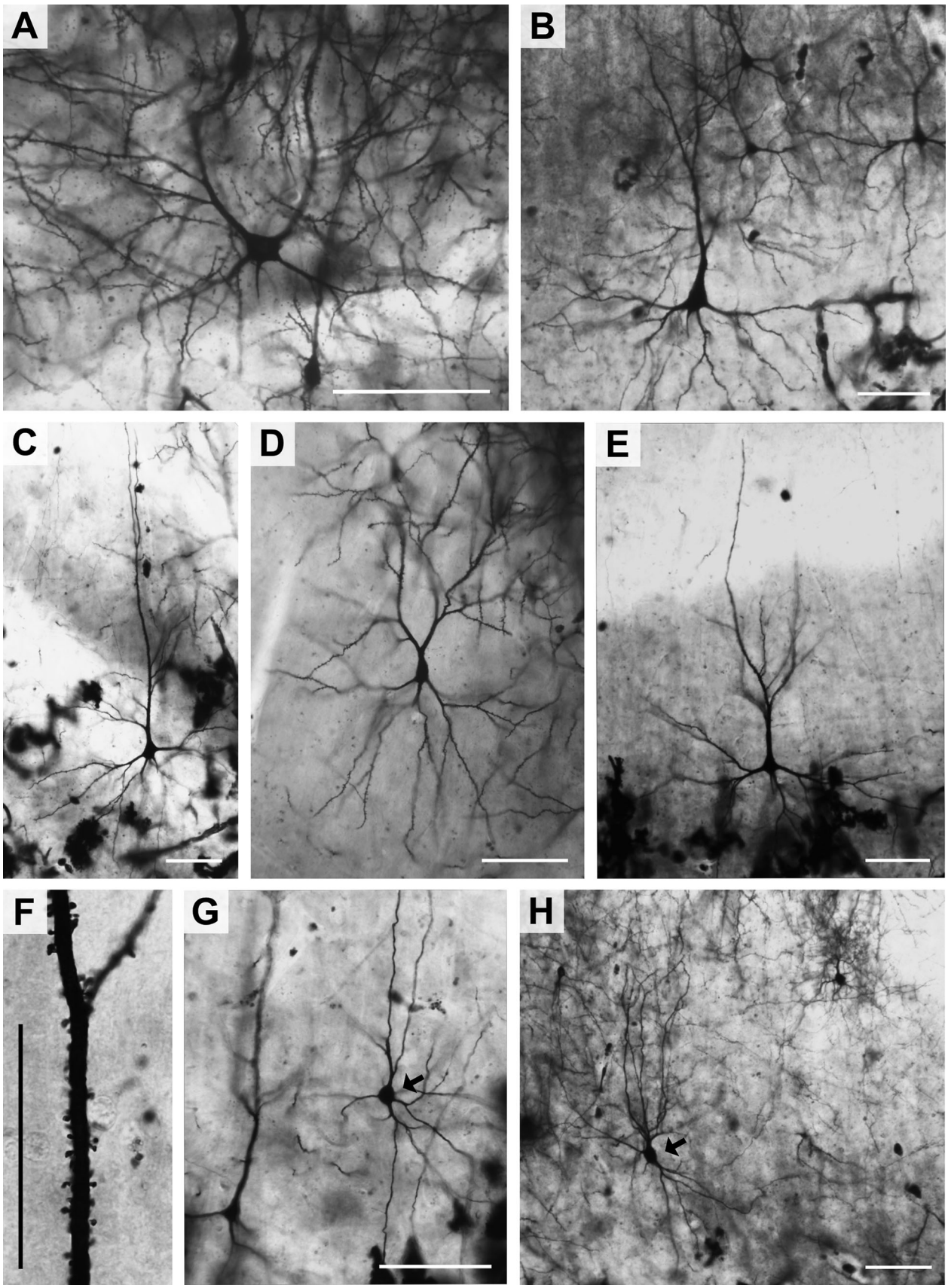

Figure 4. Photomicrographs of Golgi-stained neurons in primary visual cortex of the Siberian tiger: extraverted pyramidal (**A,D**), typical pyramidal (**B,C,E,F**), and aspiny (**G,H,** arrows) neurons. Scale bar = 100 μm in **A–E,G,H**; 50 μm in **F**.

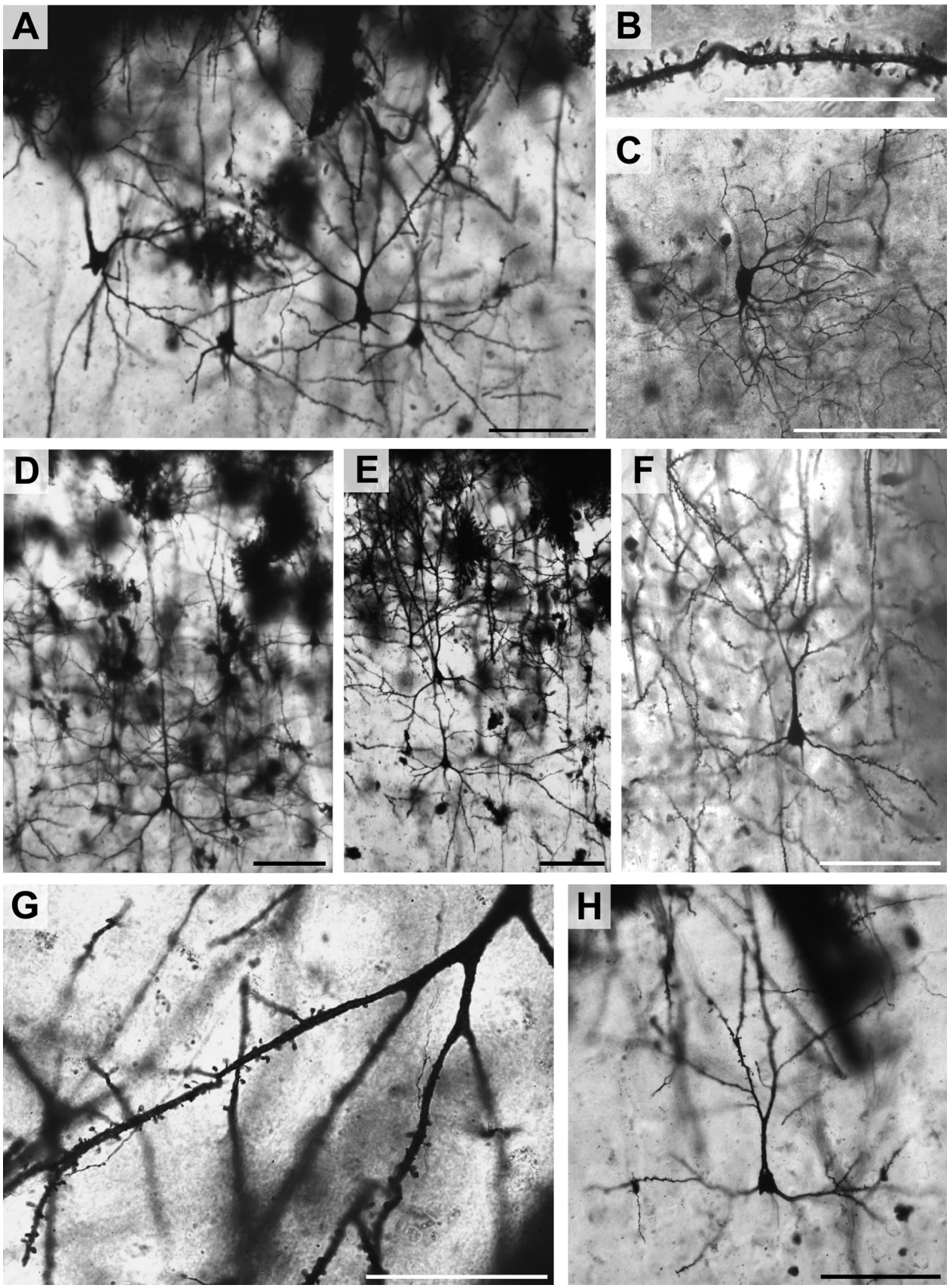

Figure 5. Photomicrographs of Golgi-stained neurons in primary motor (**A,C,F–H**), prefrontal (**B**), and primary visual (**D,E**) cortices of the clouded leopard: typical pyramidal (**A,D–H**; **B,G**, basilar dendrites) and neurogliaform (**C**) neurons. Scale bar = 100 μm in **A,C–F,H**; 50 μm in **B,G**.

TABLE 2.

Summary Statistics (Mean ± SD) for Each Neuron Type Quantified in Prefrontal, Primary Motor, and Primary Visual Cortices of the Siberian Tiger and Clouded Leopard

Species, region, neuron type	No.[1]	Vol[2]	TDL[3]	MSL[3]	DSC[4]	DSN[5]	DSD[6]	Soma size[7]	Soma depth[8]
Siberian tiger									
Frontal									
Aspiny	5	5,918 ± 2,586	3,145 ± 1,439	97 ± 29	34 ± 18	–	–	258 ± 64	667 ± 116
Extraverted	5	12,867 ± 4,224	5,966 ± 807	83 ± 10	73 ± 13	3,782 ± 1,047	0.36 ± 0.14	366 ± 76	528 ± 137
Neuroglial	1	3,787	3,770	50	76	–	–	217	728
Pyramidal	12	14,905 ± 4,703	5,278 ± 1,496	93 ± 21	60 ± 24	2,876 ± 867	0.55 ± 0.11	367 ± 103	877 ± 341
Motor									
Aspiny	6	11,645 ± 7,192	3,572 ± 1,045	104 ± 17	34 ± 7	–	–	432 ± 134	1,313 ± 311
Extraverted	2	9,667 ± 4,471	4,907 ± 1,487	80 ± 7	61 ± 13	2,344 ± 1,354	0.46 ± 0.14	335 ± 16	634 ± 107
Gigantopyramidal	3	167,069 ± 87,125	7,475 ± 3,514	148 ± 11	51 ± 24	1,098 ± 388	0.16 ± 0.05	4,028 ± 196	1,573 ± 111
Inverted	3	12,485 ± 7,894	4,633 ± 244	81 ± 11	58 ± 10	1,394 ± 335	0.30 ± 0.09	363 ± 46	1,920 ± 63
Pyramidal	10	17,379 ± 11,570	5,666 ± 1,237	86 ± 20	68 ± 18	1,874 ± 986	0.33 ± 0.11	386 ± 184	961 ± 435
Visual									
Aspiny	6	13,517 ± 5,549	4,253 ± 1,161	92 ± 22	47 ± 11	–	–	551 ± 248	1,028 ± 485
Extraverted	3	12,756 ± 8,266	5,349 ± 2,109	60 ± 6	90 ± 40	2,449 ± 1,117	0.45 ± 0.10	406 ± 49	540 ± 101
Horizontal	1	3,151	3,074	67	46	948	0.31	192	920
Inverted	1	4,652	4,352	56	78	1,247	0.29	334	1,096
Neuroglial	2	1,558 ± 141	1,600 ± 115	65 ± 6	25 ± 4	–	–	180 ± 7	630 ± 14
Pyramidal	12	22,806 ± 12,544	5,862 ± 1,846	70 ± 14	86 ± 29	1,428 ± 430	0.26 ± 0.09	598 ± 419	980 ± 104
Clouded leopard									
Frontal									
Aspiny	6	3,781 ± 1,706	1,743 ± 307	72 ± 8	24 ± 3	–	–	287 ± 112	1,015 ± 409
Extraverted	3	5,249 ± 1,818	2,589 ± 440	43 ± 13	61 ± 7	1,315 ± 626	0.49 ± 0.15	265 ± 22	539 ± 99
Inverted	2	7,480 ± 14	3,841 ± 157	58 ± 2	66	1,365 ± 57	0.36	306 ± 33	1,307 ± 122
Magnopyramidal	3	28,818 ± 9,982	1,386 ± 388	37 ± 3	37 ± 7	410 ± 44	0.31 ± 0.06	1,529 ± 62	762 ± 96
Neuroglial	1	1,904	1,459	43	34	–	–	189	1,065
Pyramidal	23	5,589 ± 1,935	3,031 ± 932	51 ± 13	62 ± 21	1,091 ± 540	0.35 ± 0.09	276 ± 61	914 ± 385
Motor									
Aspiny	8	7,060 ± 3,913	2,409 ± 1,126	76 ± 11	31 ± 13	–	–	408 ± 166	1,084 ± 181
Extraverted	3	5,278 ± 3,056	2,507 ± 161	64 ± 16	42 ± 15	1,324 ± 131	0.53 ± 0.07	252 ± 76	444 ± 84
Gigantopyramidal	3	51,871 ± 16,485	1,119 ± 424	54 ± 15	20 ± 4	272 ± 131	0.24 ± 0.06	3,882 ± 769	1,414 ± 137
Horizontal	1	4,257	1,624	71	23	256	0.16	273	1,841
Inverted	3	7,806 ± 2,529	3,548 ± 1,275	59 ± 16	59 ± 6	1,354 ± 1,087	0.35 ± 0.18	364 ± 117	1,572 ± 269
Multiapical	1	10,202	4,561	62	74	1,070	0.23	286	1,058
Neuroglial	2	2,639 ± 518	3,081 ± 420	41 ± 2	75 ± 14	–	–	199 ± 12	894 ± 225
Pyramidal	23	6,421 ± 2,630	3,287 ± 766	61 ± 13	54 ± 11	1,127 ± 322	0.35 ± 0.09	282 ± 59	841 ± 393
Visual									
Aspiny	7	2,913 ± 1,148	1,929 ± 484	60 ± 11	32 ± 7	–	–	252 ± 85	846 ± 210
Extraverted	2	4,213 ± 1,133	2,374 ± 962	40 ± 6	58 ± 15	927 ± 314	0.40 ± 0.03	295 ± 33	341 ± 71
Horizontal	1	1,830	2,297	53	43	871	0.38	193	1,195
Magnopyramidal	3	21,604 ± 2,834	1,126 ± 112	76 ± 43	17 ± 6	211 ± 45	0.19 ± 0.06	1,138 ± 178	1,096 ± 348

TABLE 2. *Continued*

Species, region, neuron type	No.[1]	Vol[2]	TDL[3]	MSL[3]	DSC[4]	DSN[5]	DSD[6]	Soma size[7]	Soma depth[8]
Multiapical	1	2,437	1,539	57	27	557	0.36	239	1,296
Neuroglial	1	1,847	1,866	52	36	–	–	154	1,106
Pyramidal	25	6,551 ± 4,800	2,837 ± 646	55 ± 9	52 ± 10	856 ± 293	0.31 ± 0.09	271 ± 124	934 ± 331

[1]Number of neurons traced.
[2]Volume in μm^3.
[3]Length in µm (TDL, total dendritic length; MSL, mean segment length).
[4]Number of segments per neuron (DSC, number of dendritic segments).
[5]Number of spines per neuron (DSN, total number of spines on dendritic segments).
[6]Number of spines per µm of dendritic length (DSD, average number of spines per µm of dendritic length).
[7]Soma size in μm^2.
[8]Soma depth in µm from the pial surface.

measures using Multivariate Adaptive Regression Splines (MARSplines; Statistica, release 12; StatSoft, Austin, TX; Friedman, 1991; Hastie et al., 2009), a nonparametric approach that is robust to violations of normality and extreme differences in variability (for details of this technique, see Jacobs et al., 2014, 2015b).

The MARSpline analysis was limited to a maximum of 10 basis functions, which allows a regression solution that, unlike a conventional two-dimensional regression that predicts *y* from *x*, can predict in up to 10 dimensions. Third-degree interactions were chosen to enable combinations of up to three variables (e.g., DSD, MSL, and TDL) to be used in the underlying equations. The analysis was performed with a penalty of one, where the penalty controls the number of dimensions the analysis can add to solve the problem. Pruning removes relatively less predictive elements of the equations, and a low value for threshold supports the addition of more dimensions. A threshold of 0.0005 and no pruning was used to facilitate a multidimensional analysis to account for correlation within species. MARSplines was used to evaluate whether any of the dendritic measures, either singularly or in combination, could differentiate between the two felid species. A Fisher exact test framework was used to calculate a χ^2 to test the null hypothesis of no difference between species. In addition, an R-square was computed to characterize the amount of differential variability between species that could be accounted for by the dendritic measures. A simple accuracy measure based on correct and incorrect classifications was then calculated.

RESULTS

Overview

Cytoarchitectural characteristics of the three cortical regions are provided in Figure 2. Overall cortical thickness was greater in the Siberian tiger than in the clouded leopard (Table 1). Layer I was thicker in the Siberian tiger than in the clouded leopard. For prefrontal and primary motor cortices, layer III was also thicker in the Siberian tiger. For both species, layer IV was present in the primary visual cortex (Fig. 2C,F), but not in the primary motor cortex (Fig. 2B,E). In the prefrontal cortex, layer IV was indistinct in the Siberian tiger (Fig. 2D), but was clearly present in the clouded leopard (Fig. 2A). In layer VI of clouded leopard visual cortex (Fig. 2C), there was also evidence of neuronal aggregations, or Rindenkerne (Dexler, 1913; DeFelipe et al., 2002). Photomicrographs of Golgi-stained tissue revealed the relatively high-quality impregnation observed in both species (Fig. 3, Siberian tiger prefrontal and primary motor cortices; Fig. 4, Siberian

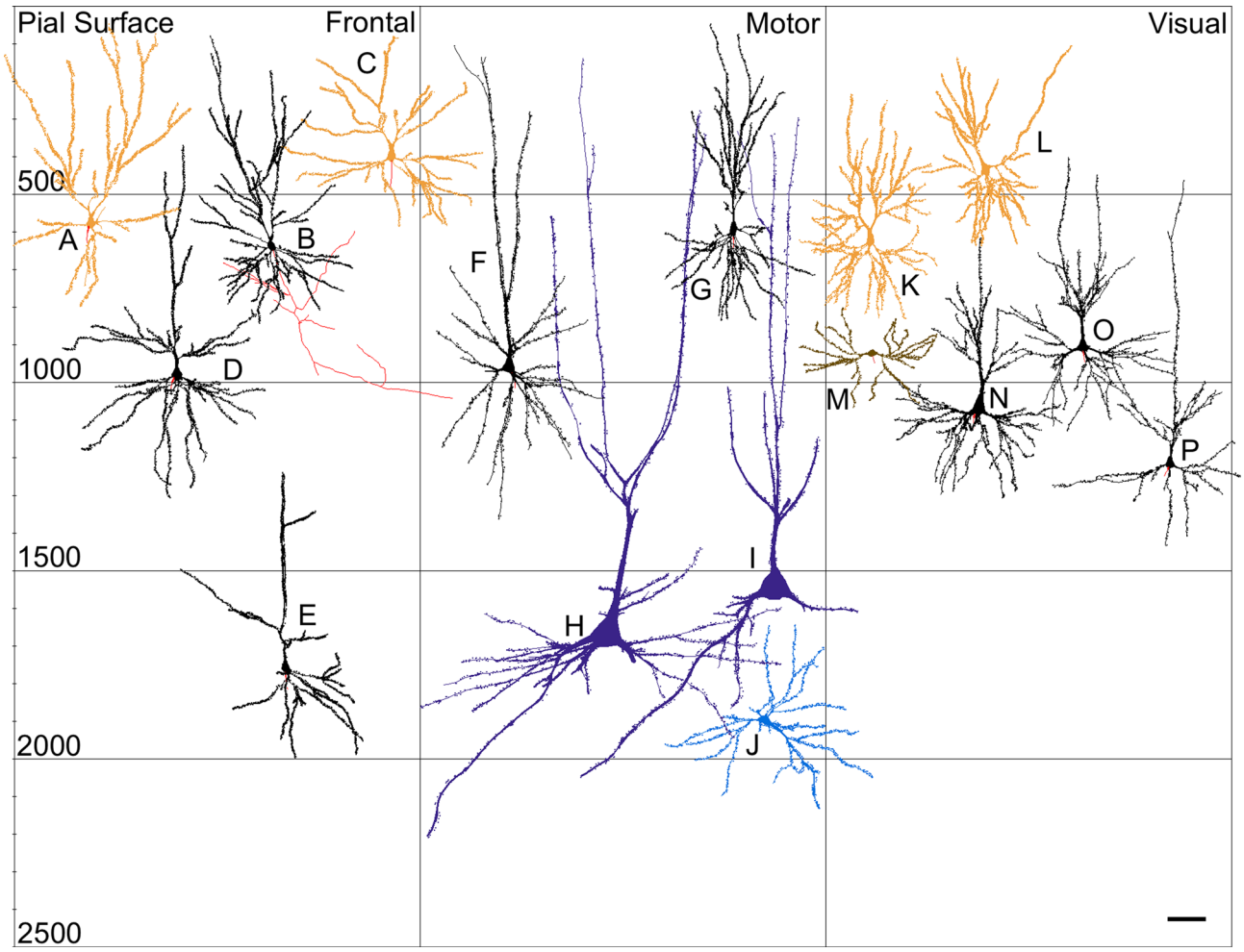

Figure 6. Neurolucida tracings of spiny projection neurons in prefrontal (**A–E**), primary motor (**F–J**), and primary visual (**K–P**) cortices of the Siberian tiger: extraverted pyramidal (**A,C,K,L**), typical pyramidal (**B,D–G,N–P**), gigantopyramidal (**H,I**), inverted pyramidal (**J**), and horizontal pyramidal (**M**) neurons. Note the extremely large size of the gigantopyramidal neurons, and the descending taproot dendrites (**H,I**). Scale bar = 100 μm. [Color figure can be viewed in the online issue, which is available at wileyonlinelibrary.com.]

tiger primary visual cortex; Fig. 5, clouded leopard prefrontal, primary motor, and primary visual cortices). Quantitative measures for all traced neuron types between species and across cortical regions are presented in Table 2. Overall, the most numerically predominant neuron type was the pyramidal neuron. Spiny neuron tracings are illustrated separately for the Siberian tiger (Fig. 6) and clouded leopard (Fig. 7), with typical, extraverted, inverted, magnopyramidal, gigantopyramidal, horizontal, and multiapical morphologies represented. Aspiny neuron tracings from both species are combined in Figure 8, with bitufted, multipolar, neurogliaform, and bipolar morphologies represented. Mean values for dependent measures of typical pyramidal neurons in both species across cortical regions are provided in Figure 9, with Sholl analyses for all neuron types displayed in Figure 10.

Spiny neurons

Typical pyramidal neurons

These neurons were the most frequently traced across all cortical areas for both the Siberian tiger (Figs. 3C, 4B,C,E,F, 6B,D–G,N–P) and the clouded leopard (Figs. 5A,B,D–H, 7C–F,H,J–L,R–V). Somata (average depth range: 841–980 μm; Table 2) were characterized by a triangular or elongated shape, with a singular, branching apical dendrite ascending toward the pial surface, and a diffuse basilar dendritic skirt. The average number of primary basilar dendrites was 4.09 ± 1.27, and the average DSD ranged from 0.26 to 0.55 (Table 2). In general, Siberian tiger neurons were noticeably larger than clouded leopard neurons in terms of Vol (by 197%), TDL (by 84%), MSL (by 49%), DSC (by 28%), and soma size (by 64%). For both species, Sholl analyses (Fig. 10A,H) demonstrated a relatively high number of

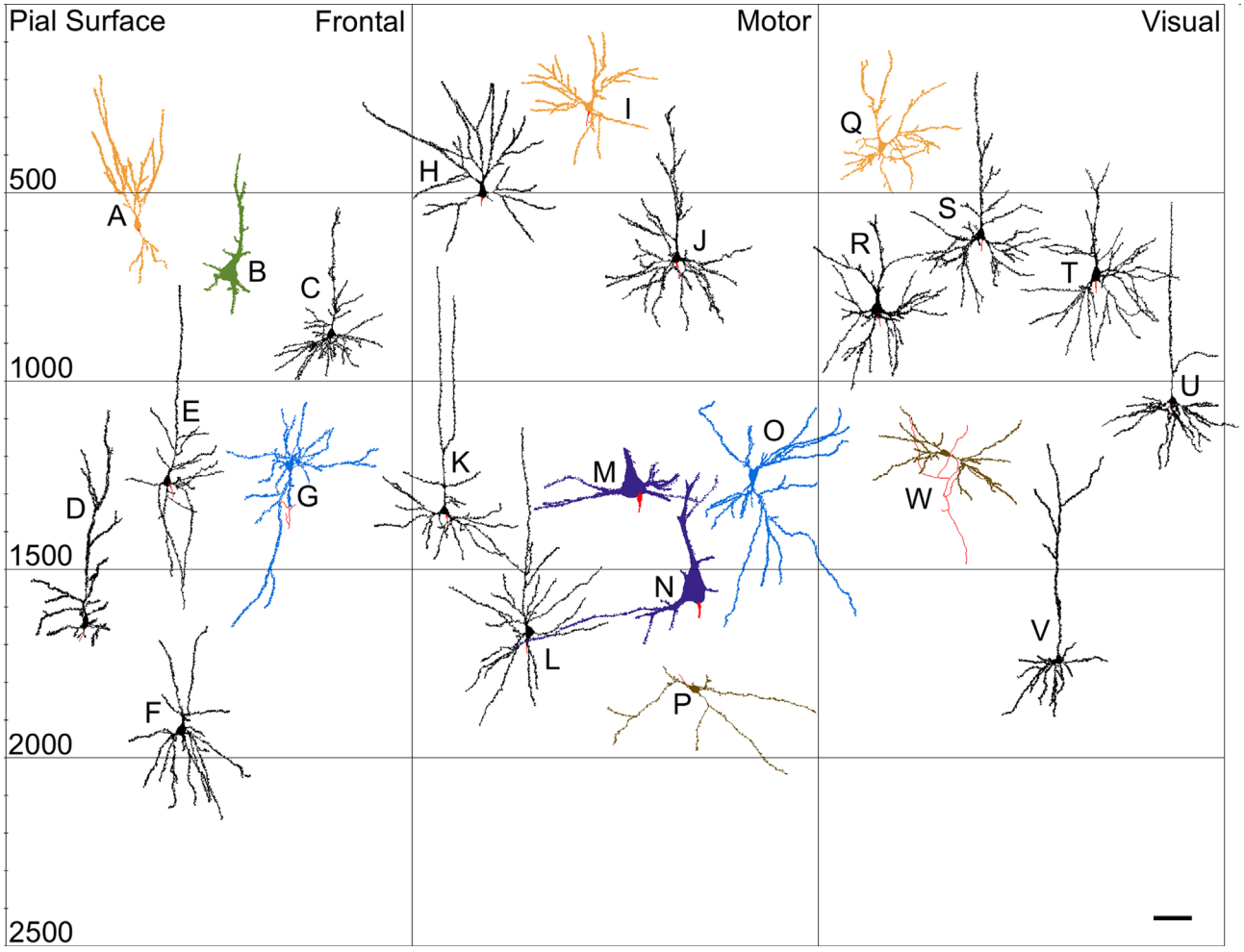

Figure 7. Neurolucida tracings of spiny neurons in prefrontal (**A–G**), primary motor (**H–P**), and primary visual (**Q–W**) cortices of the clouded leopard: extraverted pyramidal (**A,I,Q**), magnopyramidal (**B**), typical pyramidal (**C–F,H,J–L,R–V**), inverted pyramidal (**G,O**), gigantopyramidal (**M,N**), and horizontal pyramidal neurons (**P,W**). Note the incomplete tracings of both the magnopyramidal (**B**) and the gigantopyramidal (**M,N**) neurons. Scale bar = 100 μm. [Color figure can be viewed in the online issue, which is available at wileyonlinelibrary.com.]

dendritic intersections, with more extensive basilar than apical branching near (<200 μm) the soma. Basilar branching tapered off at ~400 μm, and apical branching extended to ~700–1,000 μm. These pyramidal neurons were also used in analyses of regional cortical and species differences, as explained in more detail below.

Extraverted pyramidal neurons

These neurons were traced in all cortical areas for both the Siberian tiger (Figs. 3E,G, 4A,D, 6A,C,K,L) and the clouded leopard (Fig. 7A,I,Q). These were the most superficial of all traced neuron types, with an average soma depth range of 341–634 μm (Table 2). Somata were circular or triangular in shape, with two distinct apical projections that bifurcated at or near the soma. The average number of primary basilar dendrites was 3.22 ± 1.11, and the average DSD ranged from 0.36 to 0.53. In general, Siberian tiger neurons were larger than clouded leopard neurons for most dependent measures: Vol (by 144%), TDL (by 122%), MSL (by 50%), DSC (by 42%), and soma size (by 39%). Extraverted pyramidal neurons tended to be more spinous (DSN, by 66%; DSD, by 48%) and smaller (Vol, by 13%) than typical pyramidal neurons. Sholl analyses (Fig. 10D,L) indicated greater dendritic extent in the Siberian tiger, with intersections peaking near (<200 μm) the soma in both species.

Magnopyramidal neurons

These neurons were traced in prefrontal and primary visual cortices, and were only stained in the clouded leopard (Fig. 7B). Magnopyramidal neurons (average soma depth range: 762–1,096 μm; Table 2) were characterized by an enlarged triangular soma with a

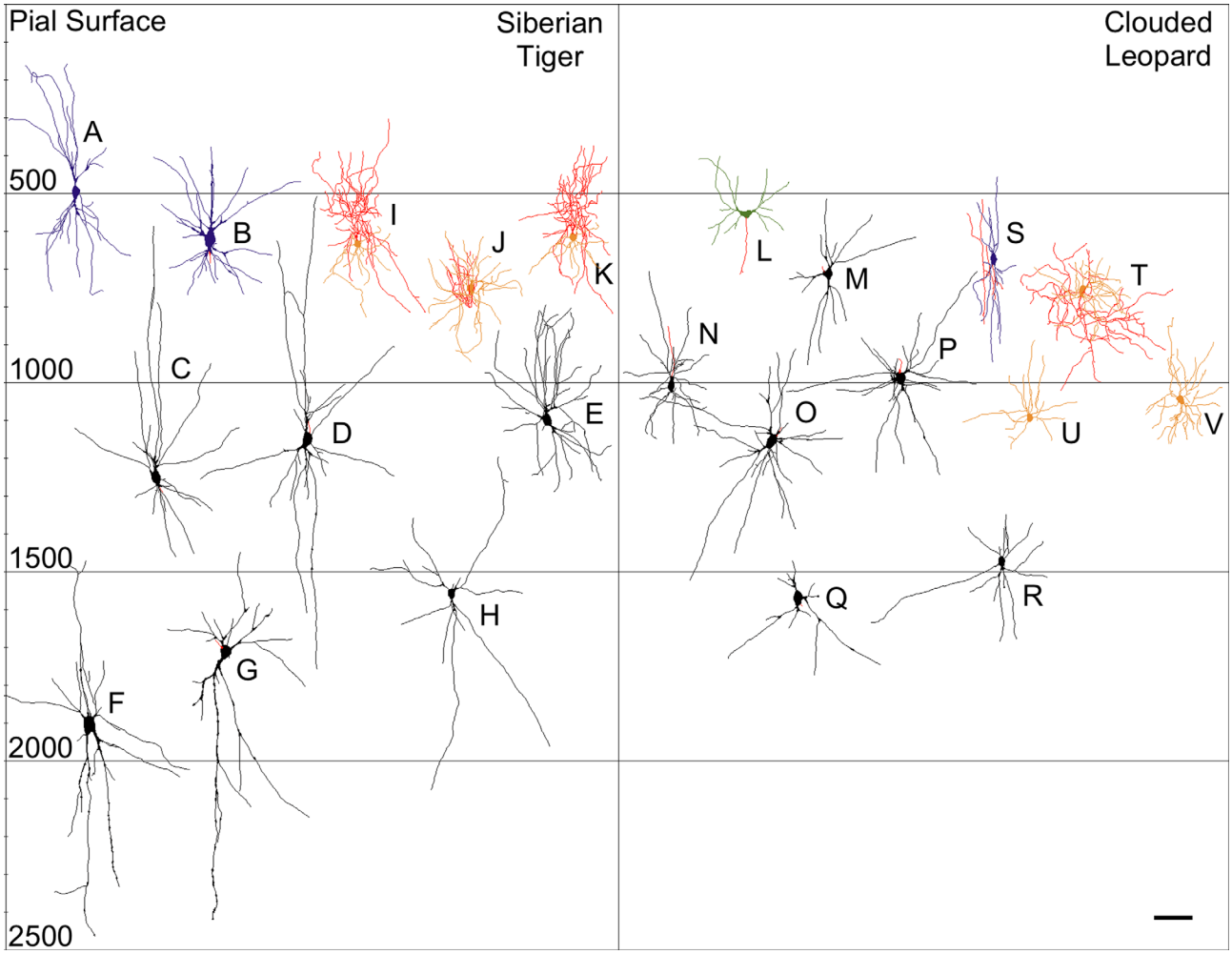

Figure 8. Neurolucida tracings of aspiny, local circuit neurons in the Siberian tiger (**A–K**; prefrontal: **A,J**; motor: **C,D,G,H**; visual: **B,E,F,I,K**) and clouded leopard (**L–V**; prefrontal: **M,Q,R**; motor: **O,P,T,V**; visual: **L,N,S,U**): aspiny bitufted (**A,B,S**), aspiny multipolar (**C–H,M–R**), neurogliaform (**I–K,T–V**), and aspiny bipolar (**L**) neurons. Scale bar = 100 μm. [Color figure can be viewed in the online issue, which is available at wileyonlinelibrary.com.]

singular, ascending apical dendrite and diffuse basilar skirt. Primary basilar dendrites averaged 5.17 ± 2.4, the most of any neuron type studied, and the average DSD ranged from 0.19 to 0.31. Magnopyramidal neurons tended to be substantially larger than typical pyramidal neurons in terms of soma size (by 299%). Due to the small number of neurons traced and the obvious incompleteness of dendritic arbors (Fig. 7B), further comparisons between cell types were not feasible. A Sholl analysis (Fig. 10J) of this neuron type follows the trend seen in other neurons, although values were attenuated due to sectioning.

Gigantopyramidal neurons

These neurons were located in layer V of the primary motor cortex in both the Siberian tiger (Figs. 3B,F, 6H,I) and the clouded leopard (Fig. 7M,N). Gigantopyramidal neurons (average soma depth range: 1,414–1,573 μm; Table 2) possessed a very enlarged soma, a single, ascending apical dendrite, and a mostly descending basilar dendritic skirt that sometimes exhibited a single taproot dendrite (Scheibel and Scheibel, 1978a). These neurons possessed, on average, 3.17 ± 1.17 primary basilar dendrites. DSD ranged from 0.16 to 0.24. Gigantopyramidal neurons were substantially larger than both magnopyramidal neurons (soma size, by 197%) and typical pyramidal neurons (soma size, by 1,084%). As with magnopyramidal neurons, further comparisons across dependent measures and between species were not possible due to dendritic sectioning. Sholl analyses (Fig. 10B,I) revealed a sizable difference between clouded leopard and Siberian tiger dendritic extent, although these values are attenuated.

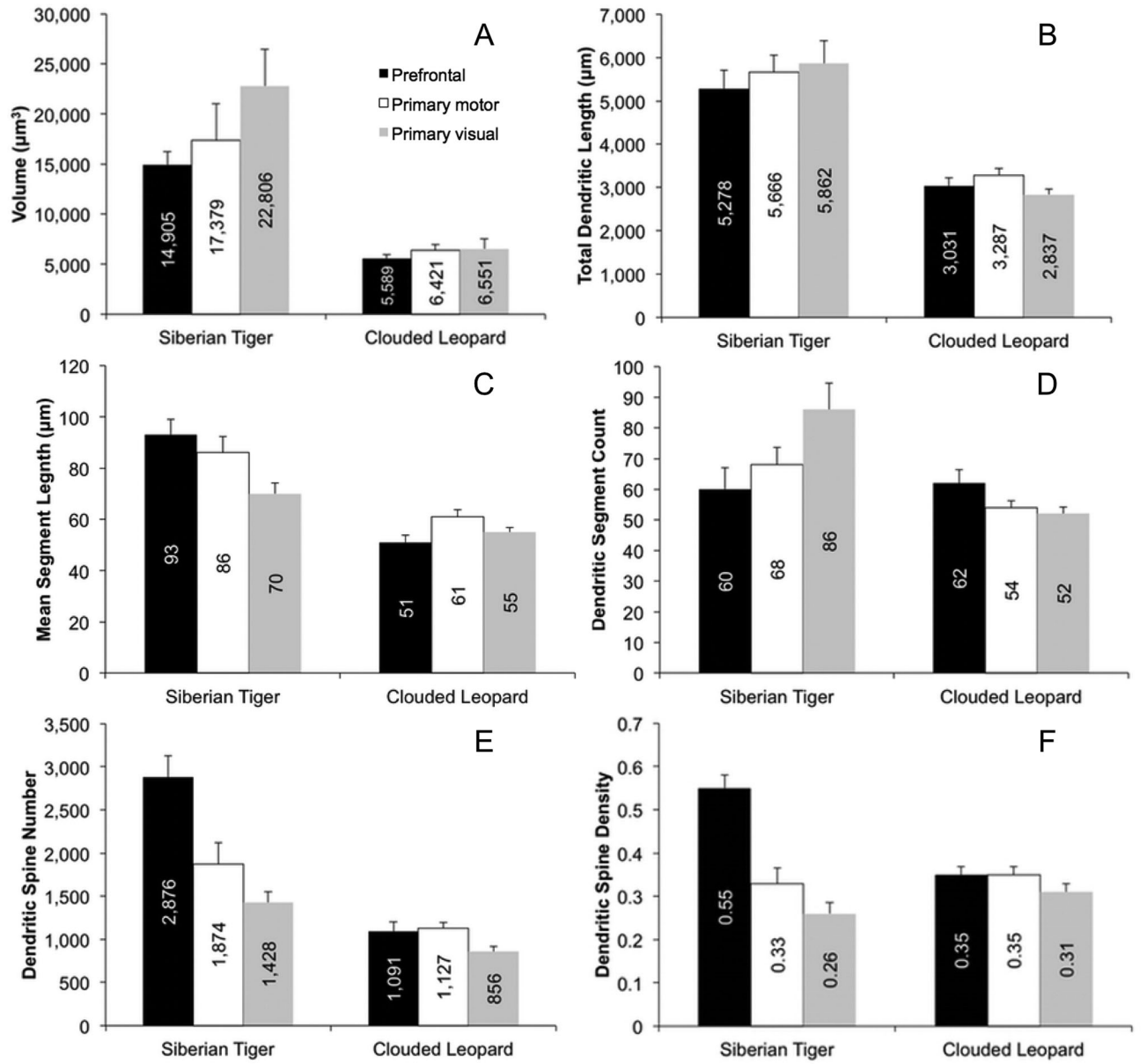

Figure 9. Mean values of dependent measures (Vol, **A**; TDL, **B**; MSL, **C**; DSC, **D**; DSN, **E**; DSD, **F**) for typical pyramidal cells across prefrontal, primary motor, and primary visual cortices in the Siberian tiger and clouded leopard. Note that the dependent measures tended to be greater across all cortical regions for the Siberian tiger than for the clouded leopard. See text for details. Error bars represent SEM.

Multiapical pyramidal neurons

These neurons were traced in clouded leopard motor and visual cortices. Averaged soma depth ranged from 1,058 to 1,296 µm (Table 2). Multiapical pyramidal neurons displayed several apical projections that extended toward the pial surface, with an extensive basilar skirt similar to that found in typical pyramidal neurons. Primary basilar dendrites averaged 3.50 ± 0.71, and DSD ranged from 0.23 to 0.36. Sholl analysis (Fig. 10M) revealed branching tapering off at ~400 µm, although the limited number of traced neurons is again problematic. Because no multiapical pyramidal neurons were traced in the Siberian tiger, dependent measure comparisons between felid species were not possible.

Inverted pyramidal neurons

These neurons were traced in all cortical areas for both the Siberian tiger (Fig. 6J) and the clouded leopard (Fig. 7G,O). They were the deepest neuron traced, with an average soma depth range of 1,096–1,920 µm (Table 2). Inverted pyramidal neurons displayed a triangular soma with a descending apical dendrite. The average number of primary basilar dendrites was 4.33 ± 1.41, and the average DSD ranged from 0.29 to 0.35.

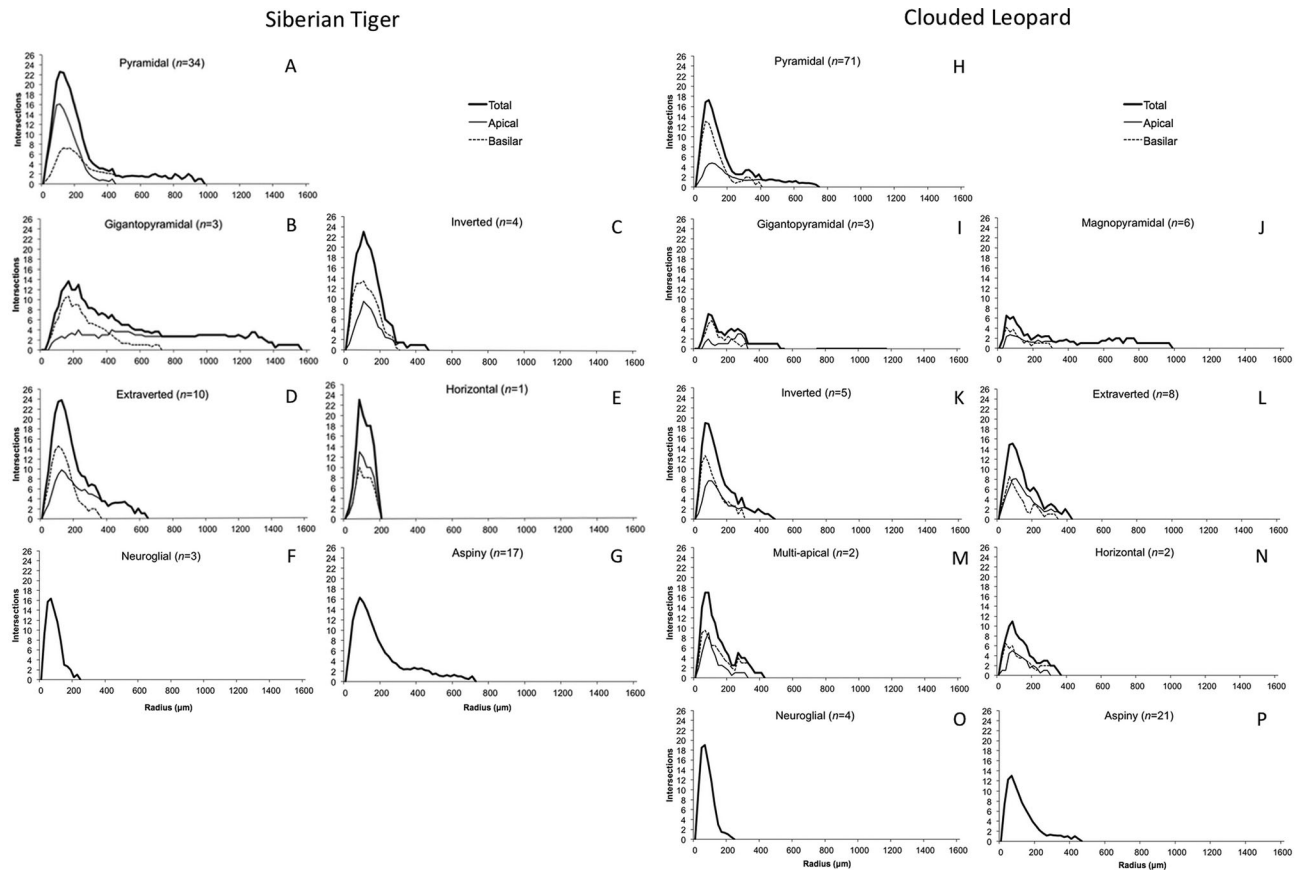

Figure 10. Sholl analyses indicating the relative branching complexity of apical, basilar, and total dendrites for Siberian tiger (**A–G**) and clouded leopard (**H–P**) neurons. The Sholl analysis quantified dendritic branching at 20-µm intervals from the soma. Seven spiny (A–E; H–N) and two aspiny (F,G,O,P) neuron types are included.

Siberian tiger neurons were generally larger than clouded leopard neurons in terms of Vol (by 37%), TDL (by 24%), MSL (by 27%), DSC (by 2%), and soma size (by 4%). However, Siberian tiger inverted pyramidal neuron spine density was less (DSD, by 15%) than that of clouded leopard inverted pyramidal neurons, with virtually no difference in DSN. Inverted pyramidal neurons were generally smaller (Vol, by 12%) and less spinous (DSN, by 0%; DSD, by 6%) than typical pyramidal neurons. Sholl analyses (Fig. 10C,K) indicated comparable dendritic extent between species, with intersections peaking near (<200 µm) the soma. Branching tapered off closer to the soma than either typical or extraverted pyramidal branching, at ~500 µm.

Horizontal pyramidal neurons

These neurons were traced in Siberian tiger primary visual cortex (Fig. 6M) and in clouded leopard primary motor and primary visual cortices (Fig. 7P,W). Horizontal pyramidal neurons were characterized by small, oblong somata (average soma depth range: 920–1,841 µm; Table 2) with dendrites projecting from each pole on the horizontal plane. Dendritic skirts displayed an average of 2.33 ± 1.53 primary basilar dendrites, and the DSD ranged from 0.16 to 0.38. Siberian tiger horizontal neurons were larger (Vol, by 4%; TDL, by 57%; MSL, by 8%; DSC, by 39%; soma size, by 15%) and more spinous (DSN, by 68%; DSD, by 15%) than clouded leopard horizontal neurons. Sholl analyses (Fig. 10E,N) indicated a substantial difference between species in terms of dendritic extent, although the small number of neurons traced makes further inferences problematic.

Nonspiny interneurons

Aspiny neurons

These neurons were traced in all cortical areas for both the Siberian tiger (Figs. 3A, 4G,H, 8A–H) and the clouded leopard (Fig. 8L–S). Average soma depth ranged from 667 to 1,313 µm (Table 2), and neurons displayed an average of 5.42 ± 1.83 primary dendritic segments. Aspiny neurons were further subdivided into

1) bitufted neurons (Fig. 8A,B,S), characterized by a relatively superficial depth and thick dendritic branching emanating vertically from polar ends of the soma; 2) multipolar neurons (Fig. 8C–H,M–R), characterized by diffuse dendritic projections from the soma; and (3) bipolar neurons (Fig. 8L), characterized by superficial depth and two primary dendritic projections at polar ends of the soma. On average, Siberian tiger aspiny neurons were larger (Vol, by 124%; TDL, by 79%; MSL, by 42%; DSC, by 30%; soma size, by 32%) than clouded leopard aspiny neurons. Sholl analyses (Fig. 10G,P) indicated that aspiny neurons were among the least complex in terms of dendritic extent.

Neurogliaform cells

These neurons were traced in all cortical areas for the Siberian tiger (Figs. 3D, 8I–K) and the clouded leopard (Figs. 5C, 8T–V). Average soma depth ranged from 630 to 1,106 μm (Table 2), and neurons displayed an average of 6.29 ± 1.50 primary dendritic segments, the most of any neuron type. Neurogliaform cells exhibited a dense dendritic plexus, which extended from the soma in all directions. Siberian tiger neurogliaform neurons were generally larger than those in clouded leopard in terms of Vol (by 2%), MSL (by 34%), and soma size (by 4%), and smaller than clouded leopard neurons in terms of TDL (by 2%) and DSC (by 24%). Sholl analyses (Fig. 10F,O) indicated comparable extent between species, with high branching close to the soma (~100 μm).

Regional cortical and interspecies dendritic variation

To examine potential regional dendritic and spine differences, only typical pyramidal neurons ($n = 105$) were considered because they were the most frequently traced neuron. Descriptive results for both species across prefrontal, primary motor, and primary visual cortices are provided in Figure 9. Although it was hypothesized that pyramidal neurons in prefrontal cortex would be more extensive than pyramidal neurons in other regions, this was not the case for all dendritic/spine measures. Regional differences appeared to be larger in the Siberian tiger than in the clouded leopard, but there was no consistent pattern between species. In the Siberian tiger, prefrontal cortex pyramidal neurons were more extensive than in other regions for only three measures: MSL, DSN, and DSD. In the clouded leopard, regional differences appeared to be minimal for all dependent measures.

Despite these mixed results for regional differences in dendritic/spine extent, pyramidal neurons were consistently more complex in the Siberian tiger than in the clouded leopard (Fig. 9), an observation supported by inferential statistics. In fact, the results from the MARSplines analysis rejected the null hypothesis of no differentiation in dendritic measures between species, $\chi^2_{(1)} = 71.36$, $p \leq 0.0001$. This procedure also provided a qualitative assessment of the relative importance of each predictor (i.e., Vol, TDL, soma size, etc.) in identifying whether a neuron belonged or did not belong to a particular species. Importance was measured by counting the number of times each neuronal variable was used by the regression analyses. The relative importance of each dendritic measure in the MARSplines analysis was as follows: Vol and TDL = 4; DSC = 2; MSL, DSN, and DSD = 0, suggesting that Vol and TDL were particularly important predictors of dendritic differences between species. Only 7 of 105 neurons were misclassified, resulting in a 93% correct differentiation. The R-square was 0.718, indicating that over 70% of the differential variability between feline species was accounted for.

DISCUSSION

The neocortex in the Siberian tiger and clouded leopard appeared similar to what has been documented in the domestic cat, in terms of both cytoarchitecture and neuronal morphology (Kelly and van Essen, 1974; Groos et al., 1978; Deschênes et al., 1979; Lund et al., 1979; Winer and Prieto, 2001; Hutsler et al., 2005). Cytoarchitecturally, both species examined here possess an agranular motor cortex and a granular visual cortex. In prefrontal cortices, layer IV was clearly present in the clouded leopard but was indistinct in the Siberian tiger, a difference that may be due to tissue sampling insofar as prefrontal cortex is heterogeneous, possessing both granular, dysgranular (i.e., transitional), and agranular sections (Rioch, 1937; Preuss, 1995; Uylings et al., 2003). Neuronal clusters similar to those observed in layer VI of clouded leopard visual cortex have been documented, usually in sensory cortices, across a variety of other species: dugong (Dexler, 1913), manatees (Reep et al., 1989), cetaceans (Hof and Van der Gucht, 2007), pygmy hippopotamus (Butti et al., 2014), platypus (Elston et al., 1999), giraffe (DeFelipe et al., 2002), and ferret (Innocenti et al., 2002).

Observed neuronal morphology in the Siberian tiger and clouded leopard were generally consistent with that observed in the domestic cat (O'Leary, 1941; Winer, 1984a,c,, 1985; Hübener et al., 1990; Matsubara et al., 1996; Van der Gucht et al., 2005; Mellott et al., 2010). In general, there was a predominance of pyramidal neurons with singular and/or narrowly bifurcating apical dendrites that contributed to a vertically oriented

cortical architecture. Across all three cortical regions, neurons traced in the Siberian tiger generally had more extensive dendritic branching than those traced in the clouded leopard, consistent with findings that neuronal morphology positively scales with increasing brain size within a mammalian lineage (Wittenberg and Wang, 2008; Manger et al., 2013; Elston and Manger, 2014; Butti et al., 2015). Below, following a brief discussion of methodological issues, we explore the morphological findings in more detail.

Methodological considerations

The most obvious limitation of the current study is the small sample size, in terms of both available brain specimens and the number of reconstructed neurons. Nevertheless, the availability of well-preserved postmortem brain tissue from such rare species presented a unique opportunity to document neuronal morphology in larger felids. More generally, the limitations of the Golgi technique have been extensively presented elsewhere and will not be addressed again here (Williams et al., 1978; Braak and Braak, 1985; Jacobs and Scheibel, 1993, 2002; Jacobs et al., 1997, 2011, 2014, 2015a,b). Specific to the present study, limitations include: 1) underestimation of spines in light microscopy (Feldman and Peters, 1979; Horner and Arbuthnott, 1991), which diminishes actual DSN and DSD values; 2) potential decreased spine density and dendritic extent measurements as a result of fixation/storage times longer than the optimal 2–3 months (Anderson et al., 2009; Butti et al., 2014); and 3) attenuated dendritic measurements for larger cells, particularly gigantopyramidal neurons, due to 120-μm-thick sections. Additionally, Golgi impregnation quality between species may have differed insofar as perfusion-fixed tissue may show greater detail (particularly for dendritic spines) than immersion-fixed tissue (Morest and Morest, 1966; Jacobs et al., 2014).

Spiny neurons

Spiny neurons in the present study were morphologically diverse but qualitatively consistent with what has been observed in the domestic cat (Winer, 1984a,b,c, 1985; Einstein and Fitzpatrick, 1991). These morphologies included a range of pyramidal-like neurons that exhibited an ascending apical dendrite (e.g., typical pyramidal, extraverted pyramidal, magnopyramidal, gigantopyramidal, and multiapical pyramidal neurons), and neurons with atypical apical dendrite orientations (e.g., inverted and horizontal pyramidal neurons).

Typical pyramidal neurons in the present study represent prototypical examples of pyramidal morphology (e.g., Fig. 4E), with truly triangular somata, a long, vertical apical dendrite, and generally symmetrical basilar skirts. Soma size appears to be considerably larger in the examined species, especially in the Siberian tiger, than in layer V and VI pyramidal neurons in the domestic cat (Katz, 1987; Valverde, 1986; Mitani et al., 1985; Hübener et al., 1990). Typical pyramidal neurons possessed the greatest variation in soma depth of all traced neurons and displayed an apical dendrite that either ascended vertically from the soma before bifurcating or split at the soma to form a V-shaped apical projection (e.g., Fig. 6F,O). These two apical characteristics have been documented in domestic cats (Mitani et al., 1985; Gabbott et al., 1987; Yamamoto et al., 1987; Ghosh et al., 1988; Hübener et al., 1990) as well as in cetartiodactyls (e.g., pygmy hippopotamus: Butti et al., 2014; bottlenose dolphin, minke whale, humpback whale: Butti et al., 2015; giraffe: Jacobs et al., 2015a), but seem to differ slightly from the singular apical dendrite that appears typical in rodents and primates (Escobar et al., 1986; Meyer, 1987). It has also been noted in the cat and monkey that these bifurcating, candelabra-like apical dendrites often form ascending dendritic bundles (Fleischhauer, 1974; Rockland and Ichinohe, 2004). Although not apparent in the present sample, presumably because of the relatively isolated nature of stained neurons, these bundles have been documented in the widely bifurcating apical branches of pyramidal neurons in the African elephant (Jacobs et al., 2011).

In general, felid neocortex appears to be characterized by a mostly vertically oriented type of information processing, as is the rodent and primate neocortex (Valverde, 1986; Mountcastle, 1997; Innocenti and Vercelli, 2010). In the current sample, the average number of primary basilar dendrites/pyramidal neuron (4.09 $\pm$ 1.27) was less than observed in corticotectal pyramidal neurons stained with Lucifer Yellow in domestic cat visual cortex ($\sim$6–9; Hübener et al., 1990), and also less than pyramidal neurons injected with horseradish peroxidase in the cat motor cortex ($\sim$5.15; Ghosh et al., 1988). Moreover, the basilar dendrites of deep pyramidal neurons in domestic cat visual cortex appear qualitatively and quantitatively (as revealed in a Sholl analysis) to be denser and more branched than the basilar dendrites in the current sample (Deschênes et al., 1979; Katz, 1987; Hübner et al., 1990). This branching characteristic suggests that cell-packing density may be lower in larger felids than in the domestic cat, a factor that appears to differentiate basilar dendritic branching patterns between elephant and humans (Jacobs et al., 2011).

Extraverted pyramidal neurons were frequently present in layers II and III and typically displayed two apical

dendrites and a diminutive basilar dendritic skirt. These neurons have been described in the superficial cortical layers of the domestic cat (O'Leary, 1941; Ramon-Moliner, 1961b), although they have sometimes been referred to as modified pyramidal neurons (Ghosh et al., 1988). They have also been documented in a variety of other mammals, from the hedgehog, bat, and opossum (Sanides and Sanides, 1972; Valverde and Facal-Valverde, 1986; Ferrer, 1987) to larger mammals such as the pygmy hippopotamus (Butti et al., 2014) and several species of cetaceans (Ferrer and Perera, 1988; Hof and Van der Gucht, 2007; Butti et al., 2015). Although extraversion has been viewed as a more primitive characteristic of pyramidal neurons (Marin-Padilla, 1992), the prevalence of extraverted neurons in species with agranular cortex (e.g., hippopotamus and cetaceans) is suggestive of a difference in cortical processing networks (Ebner, 1969; Sanides and Sanides, 1972). In terms of relative size, extraverted pyramidal neurons in the Siberian tiger exhibited roughly the same dendritic extent (in terms of Vol and TDL) as these neurons in the giraffe (brain mass = 539 g; Jacobs et al., 2015a) and minke whale (brain mass = 1,810 g; Butti et al., 2015), even though the Siberian tiger has a substantially smaller brain.

Magnopyramidal neurons in the present sample were only found in clouded leopard neocortex. Although not specifically identified as such, potential magnopyramidal neurons have been documented in the visual cortex of the domestic cat (O'Leary, 1941; Einstein and Fitzpatrick, 1991; Winer and Prieto, 2001). More definitive descriptions have been found in the classical language regions of the human (Braak, 1978; Hayes and Lewis, 1995) and the morphometrically similar solitary cells of Meynert in primate visual cortex (Meynert 1867; Chan-Palay et al., 1974; Hof et al., 2000). Magnopyramidal soma size was much larger in the clouded leopard than in the giraffe (Jacobs et al., 2015a) or the dolphin and minke whale (Butti et al., 2015), and approached the soma size of magnopyramidal neurons in the humpback whale (Butti et al., 2015). Dendritic extent (as indicated by Vol and TDL), however, was much less in the clouded leopard than in the giraffe or minke whale (presumably due to Golgi impregnation differences among the specimens). Indeed, the relatively incomplete nature of these neurons in the present study precludes further comparison with other species. Finally, whether these neurons in the visual cortex of the clouded leopard, which does lead a largely arboreal existence, suggest greater importance of the visual system, as has been suggested for other animals (Sherwood et al., 2003), remains an open question.

Gigantopyramidal neurons, by far the largest neuron type traced in the present study, are consistent in terms of location and size with Betz cells in humans, which are found in layer Vb of primary motor cortex (Betz, 1874; Braak and Braak, 1976; Meyer, 1987). In the domestic cat, gigantopyramidal neurons have also been loosely considered to be the equivalent of primate Betz cells (Ramon-Moliner, 1961a; Hassler and Muhs-Clements, 1964; Crawford and Curtis, 1966; Kaiserman-Abramof and Peters, 1972). Betz (1874) had observed these gigantopyramidal neurons in several species of primates and in canids, an observation extended by Brodmann (1909), who documented that these gigantopyramidal neurons tend to be particularly large in carnivores (e.g., brown bear, kinkajou, lion, and tiger). The present study tentatively confirms this observation insofar as the average soma size of gigantopyramidal neurons in both species, but especially the Siberian tiger, was considerably larger than typically observed in the domestic cat (Deschênes et al., 1979; Ghosh et al., 1988). Moreover, the soma size of these neurons in the Siberian tiger are equivalent to or larger than those observed in humans (Brodmann, 1909; Sasaki and Iwata, 2001; Rivara et al., 2003; Sherwood et al., 2003), although there exists substantial variability in methodology and soma size estimates in the literature (Brodmann, 1909; Groos et al., 1978; Kaiserman-Abramof and Peters, 1972; Ghosh et al., 1988). In comparison with other species examined with the same methodology as the present study, the soma size of gigantopyramidal neurons in the Siberian tiger (4,028 $\pm$ 196 μm^2) and clouded leopard (3,882 $\pm$ 769 μm^2) are substantially larger than in the giraffe (1,184 $\pm$ 246 μm^2, Jacobs et al., 2015a) or minke whale (1,056 $\pm$ 251 μm^2, Butti et al., 2015). In terms of dendritic characteristics, the gigantopyramidal neurons in the present study appeared very similar to those described in the domestic cat (see Fig. 1 of Kaiserman-Abramof and Peters, 1972; Fig. 8 of Ghosh et al., 1988). Nevertheless, as with typical pyramidal neurons, these neurons generally exhibited fewer basilar dendrites per neurons and less dense basilar dendritic skirts than in the domestic cat (Deschênes et al., 1979; Ghosh et al., 1988). The observed circumferential dendrites and descending taproot branches are similar to those observed in humans (Scheibel and Scheibel, 1978a). Although few studies have provided three-dimensional tracings of gigantopyramidal neurons, some quantitative comparisons are possible with the caveat that these comparisons should be interpreted cautiously because of the incomplete nature of these reconstructions. In terms of dendritic volume, clouded leopard gigantopyramidal neurons (51,871 $\pm$ 16,485 μm^3) were similar to

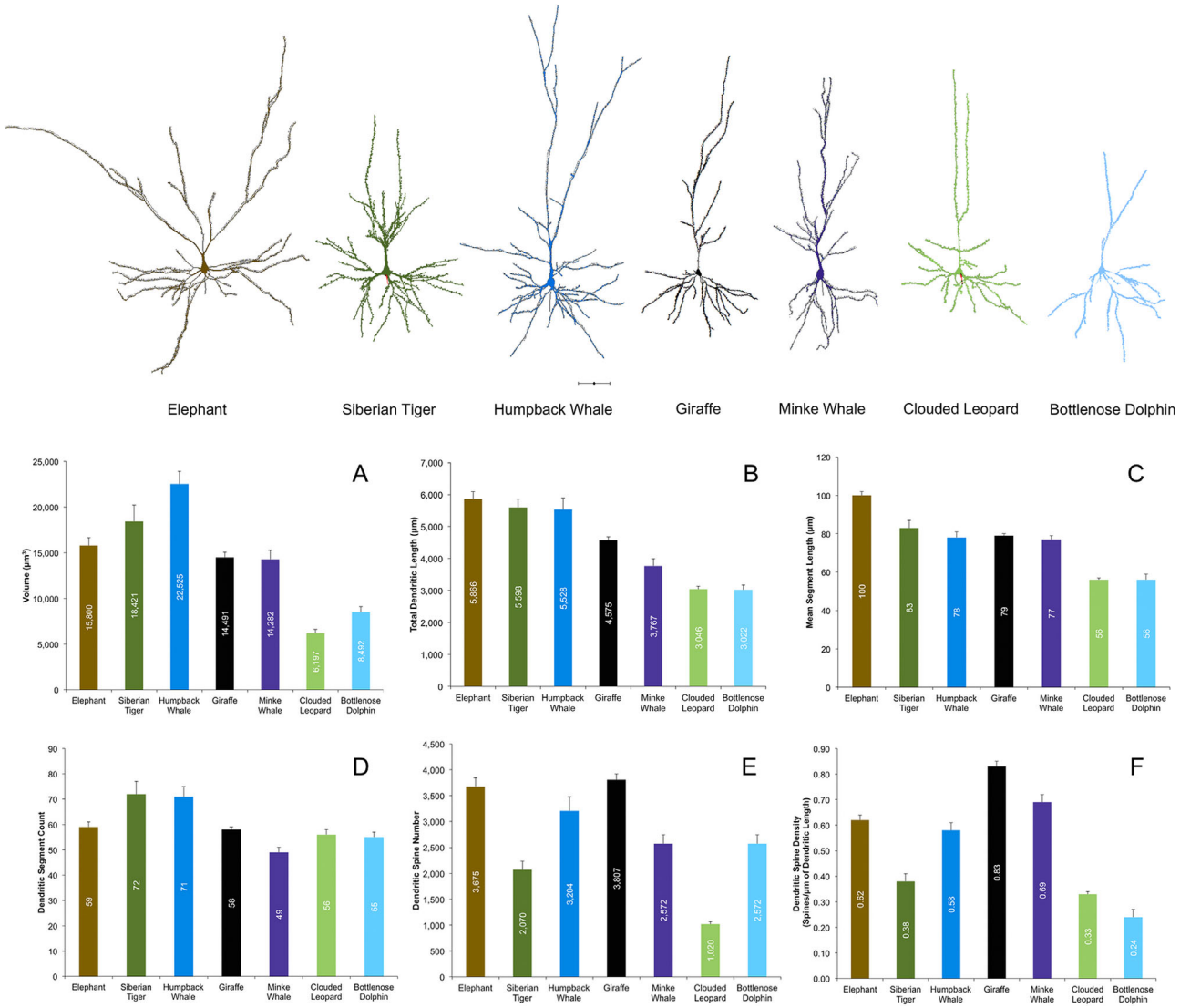

Figure 11. Qualitative and quantitative comparison of typical pyramidal neurons quantified in the same manner across several species: African elephant (brain mass = 4,990 g), Siberian tiger (brain mass = 258 g); humpback whale (brain mass = 3,603 g); giraffe (brain mass = 539 g); minke whale (brain mass = 1,810 g); clouded leopard (brain mass = 77.5 g); bottlenose dolphin (brain mass = 1,250 g). The displayed pyramidal neuron tracings were chosen for completeness of the Golgi impregnation and represent the approximate average TDL for each species. The representative pyramidal neuron tracings at the top of the figure originated in prefrontal cortex (African elephant), visual cortex (Siberian tiger, humpback whale, and minke whale), anterior temporal cortex (dolphin), and motor cortex (giraffe and clouded leopard). Graphs A-F present comparative data for six dependent measures: Vol (**A**), TDL (**B**), MSL (**C**), DSC (**D**), DSN (**E**), and DSD (**F**). The order of species in the representative tracings and graphs was determined by descending TDL values (see **B**), from the African elephant to the dolphin. See text for further discussion. Error bars represent SEM. Scale bar = 100 µm. [Color figure can be viewed in the online issue, which is available at wileyonlinelibrary.com.]

those in the giraffe (68,547 ± 33,632 µm^3, Jacobs et al., 2015a) and the minke whale (40,562 ± 6,767 µm^3; Butti et al., 2015); however, dendritic volume in Siberian tiger gigantopyramidal neurons (167,069 ± 87,125 µm^3) was much larger.

The limited number of traced *multiapical, inverted,* and *horizontal pyramidal neurons* constrains what the present study can infer about these neuron types. Multiapical pyramidal neurons, which were located in layers III and IV in the clouded leopard, have been documented in several species (rat and hedgehog: Ferrer et al., 1986a; dog: Ferrer et al., 1986b; bat: Ferrer, 1987; bottlenose dolphin and humpback whale: Butti et al., 2015), and are very common in the African elephant (Jacobs et al., 2011). Inverted pyramidal neurons, which were historically believed to be the result of faulty neuronal migration in larger brains (Van der Loos, 1965), appear to participate in local and

interhemispheric communication (Mendizabal-Zubiaga et al., 2007). They have been observed in small percentages (1–8.5%) across many species (domestic cat: Ramon-Moliner, 1961c; Ferrer et al., 1986b; Matsubara et al., 1996; rabbit: Globus and Schiebel, 1967; rodents: Steger et al., 2013; Xenarthra: Sherwood et al., 2009; minke whale: Butti et al., 2015; giraffe: Jacobs et al., 2015a; chimpanzee: Qi et al., 1999; elephant: Jacobs et al., 2011). In terms of soma size, Siberian tiger (356 ± 40 μm^2) and clouded leopard (340 ± 90 μm^2) inverted pyramidal neurons are larger than those of the domestic cat (~200 μm^2, Matsubara et al., 1996). Finally, horizontal pyramidal neurons, which may contribute to the lateral integration of cortical information (Van Brederode et al., 2000), have also been observed at varying cortical depths in several mammals (rodents: Ferrer, 1986a; dog and cat: Ferrer et al., 1986b; primates: Meyer, 1987, de Lima et al., 1990; African elephant: Jacobs et al., 2011; giraffe: Jacobs et al., 2015a; minke whale and humpback whale: Butti et al., 2015). For reasons that remain unclear, horizontal pyramidal soma size and dendritic extent in the present study were both much smaller than in cetaceans (Butti et al., 2015) and giraffes (Jacobs et al., 2015a).

Nonspiny interneurons

Aspiny neurons in the present study belonged to three nonpyramidal classes: multipolar, bipolar, and bitufted. These relatively small neurons are believed to represent 15–30% of all neurons in the neocortex (DeFelipe and Fariñas 1992), and appear to be ubiquitous in mammals (Sherwood et al., 2009), having been observed in domestic cats (Peters and Regidor, 1981; Chen et al., 1996; Winer, 1984a,b,c), rodents (Feldman and Peters, 1978), cetartiodactyls (Ferrer and Perera, 1988; Butti et al., 2015; Jacobs et al., 2015a), and afrotherians (Jacobs et al., 2011). Dendritic radius reached ~500 μm in the clouded leopard and ~800 μm in the Siberian tiger, which is greater than what is typically seen in the domestic cat (~50–400 μm; Somogyi et al., 1983; Mitani et al., 1985; Winer, 1984a,b, 1985), similar to values observed in the giraffe (~500–600 μm; Jacobs et al., 2015a), macaque monkey (~500 μm, Lund and Lewis, 1993) and human (~500–800 μm, Meyer, 1987; Kisvárday et al., 1990), but shorter than in the African elephant (~1,000 μm; Jacobs et al., 2011). The findings for *neurogliaform cells* are much the same insofar as those examined in the present study were generally larger than reported in some species (cat: Thomson and Bannister, 2003; rat, monkey: Povysheva et al., 2007), similar to those in the giraffe (Jacobs et al., 2015a), but smaller than those observed in the elephant (Jacobs et al., 2011). As with these other species, neurogliaform neurons possessed the greatest number of dendritic segments out of any traced cell type, perhaps contributing to their suggested synchronization of neuronal circuits (Simon et al., 2005; Zsiros and Maccaferri, 2005).

Quantitative comparison of pyramidal neurons across species

Direct quantitative comparisons of dendritic extent in the present study with findings in the domestic cat are difficult because past studies of the cat have provided only partial measurements (e.g., basilar dendritic field diameter or radius; Ghosh et al., 1988; Hübener et al., 1990) rather than three-dimensional reconstructions of neurons. Thus, to further our understanding of the quantitative morphological characteristics of Siberian tiger and clouded leopard neocortex, we compared the current results with those from other species quantified with the same rapid Golgi staining and neuronal reconstruction methodology. Specifically, we compared the dendritic/spine values of pyramidal neurons in the present study (Siberian tiger, $n = 34$; clouded leopard, $n = 71$) with the same measurements obtained from pyramidal neurons in several cortical regions of the following: African elephant ($n = 40$, visual and frontal cortices; Jacobs et al., 2011), giraffe ($n = 143$, motor and visual cortices; Jacobs et al., 2015a), and three cetacean species (minke whale, $n = 24$, visual and motor cortices; humpback whale, $n = 20$, visual, frontal, and temporal cortices; bottlenose dolphin, $n = 33$, visual and temporal cortices; Butti et al., 2015). Summary information for each of these species is provided in Jacobs et al. (2015a). We did not compare these dendritic measures with those obtained in our human studies (Jacobs et al., 1997, 2001) because the human research only examined the basilar dendrites of superficial pyramidal neurons. Although such comparisons are not ideal because of the number of uncontrolled factors (e.g., small sample size, subjects of different ages, regional and associated functional cortical variations, perfusion vs. immersion fixation), methodologically similar quantitative analyses provide at least a preliminary, relative measure for such cross-species comparisons.

A total of 365 pyramidal neurons were compared for dendritic (Vol, TDL, MSL, DSC) and spine (DSN, DSD) measures. To allow qualitative comparisons, sample tracings of representative neurons from each species are arranged across the top of Figure 11 by average TDL measurements (Fig. 11B). Quantitatively, the Siberian tiger was high on most dendritic measures, exhibiting values similar to the African elephant and

humpback whale (Vol: humpback whale > African elephant > Siberian tiger; TDL: African elephant > Siberian tiger > humpback whale; DSC: Siberian tiger > humpback whale > African elephant; Fig. 11A–D). By comparison, dendritic values for the clouded leopard were among the lowest, and roughly comparable to those of the bottlenose dolphin. That the Siberian tiger exhibited Vol and TDL values similar to those of the African elephant and humpback whale is noteworthy given that the Siberian tiger is substantially smaller in both brain and body size. This observation appears consistent with the hypothesis that a positive correlation exists between brain size and neuron size within mammalian lineages rather than across them (Elston and Manger, 2014). The relatively high DSC values for both the Siberian tiger and clouded leopard suggest more extensive dendritic branching in felids, similar to what is seen in cetartiodactyls (Butti et al., 2015; Jacobs et al., 2015a) but different from the fewer, longer projections common to the African elephant (Jacobs et al., 2011). Spine values for both the Siberian tiger and clouded leopard were low, perhaps reflecting less than optimal impregnation (as was the case for the dolphin; Butti et al., 2015).

CONCLUSIONS

The present findings in the Siberian tiger and clouded leopard supplement a growing database on the neuronal morphology of species beyond rodents and primates (see Neuromorpho.org). In general, neocortical neuronal morphology in these two felids appears largely consistent with what has been observed in the domestic cat, although neurons in the larger felids tended to exhibit greater dendritic extent. Two findings were particularly noteworthy: 1) the pyramidal neurons of the Siberian tiger were disproportionally large relative to body/brain size insofar as they were nearly as extensive as those observed in much larger mammals (e.g., African elephant, humpback whale); and 2) as suggested by Brodmann's (1909) previous observations, felid gigantopyramidal neurons in layer V of the motor cortex were much larger than has been observed in other species to date (e.g., domestic cats, primates, cetartiodactyls). A larger comparative study of these neurons across a much wider variety of species is currently in progress to elucidate underlying functional reasons for the large size of these gigantopyramidal neurons in felids, or carnivores in general.

ACKNOWLEDGMENTS

We thank Cheryl Stimpson for her assistance with database archiving, photo documentation, and the dissection of the brains. We also thank Dr. Mark Saviano for his continued statistical support.

CONFLICT OF INTEREST STATEMENT

The authors have no conflicts of interest.

ROLE OF AUTHORS

All authors had full access to all the data in the study and take responsibility for the integrity of the data and the accuracy of the data analysis. Study concept and design: PRM, CCS, PRH, BJ. Collection of and qualitative analysis of data: CBJ, BJ, LCW, CCS, PRH, PMR. Statistical analysis and interpretation: MS, BJ. Procurement, preparation, and fixation of tissue: AHL, MFB, PRM, CCS, JRR, MAR, TW. Obtained funding: PRM, PRH, CCS. Drafting of the manuscript: CBJ, BJ, MS, MET, MEG, NBSS. Photomicrography and preparation of figures: CBJ, LW, PRM, BJ, MET, MEG, NBSS. Critical revision of the manuscript for important intellectual content: MAR, PRM, PRH, CCS, BJ. Study supervision: BJ, PRH, PRM, CCS.

LITERATURE CITED

Anderson K, Bones B, Robinson B, Hass C, Lee H, Ford K, Roberts T-A, Jacobs B. 2009. The morphology of supragranular pyramidal neurons in the human insular cortex: a quantitative Golgi study. Cereb Cortex 19:2131–2144.

Anderson PA, Olavarria J, Van Sluyters RC. 1988. The overall pattern of ocular dominance bands in cat visual cortex. J Neurosci 8:2183–2200.

Betz W. 1874. Anatomischer Nachweis zweier Gehirncentra. Zbl Med Wiss 12:595–599.

Bok ST. 1959. Histonomy of the cerebral cortex. Amsterdam: Elsevier.

Braak H. 1978. On magnopyramidal temporal fields in the human brain—probable morphological counter parts of Wernicke's sensory speech region. Anat Embryol 152: 141–169.

Braak H, Braak E. 1976. The pyramidal cells of Betz within the cingulate and precentral gigantopyramidal field in the human brain. Cell Tissue Res 172:103–119.

Braak H, Braak E. 1985. Golgi preparations as a tool in neuropathology with particular reference to investigations of the human telencephalic cortex. Prog Neurobiol 25:93–139.

Brodmann K. 1909. Vergleichende Lokalisationlehre der Grosshirnrinde in ihren Prinzipien dargestellt auf Grund des Zellenbaues. Leipzig, Germany: J.A. Barth.

Buckley-Beason VA, Johnson WE, Nash WG, Stanyon R, Menninger JC, Driscoll CA, Howard J, Bush M, Page JE, Roelke ME, Stone G, Martelli PP, Wen C, Ling L, Duraisingam RK, Lam PV, O'Brien SJ. 2006. Molecular evidence for species-level distinctions in clouded leopards. Curr Biol 16:2371–2376.

Butti C, Fordyce RE, Raghanti MA, Gu X, Bonar CJ, Wicinsky BA, Wong EW, Roman J, Brake A, Eaves E, Spocter MA, Tang CY, Jacobs B, Sherwood CC, Hof PR. 2014. The cerebral cortex of the pygmy hippopotamus, *Hexaprotodon liberiensis* (Cetartiodactyla, Hippopotamidae): MRI, cytoarchitecture, and neuronal morphology. Anat Rec 297:670–700.

Butti C, Janeway CM, Townshend C, Wicinski BA, Reidenberg JS, Ridgway SH, Sherwood CC, Hof PR, Jacobs B. 2015. The neocortex of cetartiodactyls: I. A comparative Golgi analysis of neuronal morphology in the bottlenose dolphin (*Tursiops truncatus*), the minke whale (*Balaenoptera acutorostrata*), and the humpback whale (*Megaptera novaeangliae*). Brain Struct Funct 220:3339–3368.

Chan-Palay V, Palay SL, Billings-Gagliardi SM. 1974. Meynert cells in the primate visual cortex. J Neurocytol 3:631–658.

Chen W, Zhang J-J, Hu G-Y, Wu C-P. 1996. Electrophysiological and morphological properties of pyramidal and nonpyramidal neurons in the cat motor cortex *in vitro*. Neuroscience 73:39–55.

Crawford JM, Curtis DR. 1966. Pharmacological studies on feline Betz cells. J Physiol 186:121–138.

De Carlos, JA, Lopez-Mascaraque, L, Valverde, F. 1985. Development, morphology and topography of chandelier cells in the auditory cortex of the cat. Dev Brain Res 22:293–300.

de Lima AD, Voigt T, Morrison JH. 1990. Morphology of the cells within the inferior temporal gyrus that project to the prefrontal cortex in the macaque monkey. J Comp Neurol 296:159–172.

DeFelipe J. 2011. The evolution of the brain, the human nature of cortical circuits, and intellectual creativity. Front Neuroanat 5:29.

DeFelipe J, Fariñas I. 1992. The pyramidal neuron of the cerebral cortex: morphological and chemical characteristics of the synaptic inputs. Prog Neurobiol 39:563–607.

DeFelipe J, Alonso-Nanclares L, Arellano JI. 2002. Microstructure of the neocortex: comparative aspects. J Neurocytol 31:299–316.

Deschênes M, Labelle A, Landry P. 1979. Morphological characterization of slow and fast pyramidal tract cells in the cat. Brain Res 178:251–274.

Dexler H. 1913. Das Hirn von Halicore dugong Erxl. Gegenbaurs Morphol Jahrb 45:97–190.

Ebner FF. 1969. A comparison of primitive forebrain organization in metatherian and eutherian mammals. Ann N Y Acad Sci 167:241–257.

Einstein G, Fitzpatrick D. 1991. Distribution and morphology of area 17 neurons that project to the cat's extrastriate cortex. J Comp Neurol 303:132–149.

Elston GN. 2002. Cortical heterogeneity: implications for visual processing and polysensory integration. J Neurocytol 31:317–335.

Elston GN, Manger PR. 2014. Pyramidal cells in V1 of African rodents are bigger, more branched and more spiny than those in primates. Front Neuroanat 8:4.

Elston GN, Manger PR, Pettigrew JD. 1999. Morphology of pyramidal neurones in cytochrome oxidase modules of the S-I bill representation of the platypus. Brain Behav Evol 53:87–101.

Elston GN, Benavides-Piccione R, DeFelipe J. 2001. The pyramidal cell in cognition: a comparative study in human and monkey. J Neurosci 21:RC163.

Escobar MI, Pimienta H, Caviness VS Jr, Jacobson M, Crandall JE, Kosik KS. 1986. Architecture of apical dendrites in the murine neocortex: dual apical dendritic systems. Neuroscience 17:975–989.

Feldman ML, Peters A. 1978. The forms of non-pyramidal neurons in the visual cortex of the rat. J Comp Neurol 179: 761–793.

Feldman ML, Peters A. 1979. Technique for estimating total spine numbers on Golgi-impregnated dendrites. J Comp Neurol 118:527–542.

Ferrer I. 1987. The basic structure of the neocortex in insectivorous bats (*Miniopterus sthreibersi* and *Pipistrellus pipistrellus*). A Golgi study. J Hirnforsch 28:237–243.

Ferrer I, Fabregues I, Condom E. 1986a. A Golgi study of the sixth layer of the cerebral cortex. I. The lissencephalic brain of Rodentia, Lagomorpha, Insectivora and Chiroptera. J Anat 145:217–234.

Ferrer I, Fabregues I, Condom E. 1986b. A Golgi study of the sixth layer of the cerebral cortex. II. The gyrencephalic brain of Carnivora, Artiodactyla, and primates. J Anat 146:87–104.

Ferrer I, Perera M. 1988. Structure and nerve cell organization in the cerebral cortex of the dolphin *Stenella coeruleoalba* a Golgi study. With special attention to the primary auditory area. Anat Embryol 178:161–173.

Fleischhauer K. 1974. On different patterns of dendritic bundling in the cerebral cortex of the cat. Z Anat Entwickl Gesch 143:115–126.

Friedman JH. 1991. Multivariate adaptive regression splines. Ann Stat 19:1–67.

Gabbott PLA, Martin KAC, Whitteridge D. 1987. Connections between pyramidal neurons in layer 5 of cat visual cortex. J Comp Neurol 259:364–381.

Ghosh S, Fyffe REW, Porter R. 1988. Morphology of neurons in area 4 of the cat's cortex studied with intracellular injection of HRP. J Comp Neurol 269:290–312.

Gilbert CD, Wiesel TN. 1989. Columnar specificity of intrinsic horizontal and corticocortical connections in cat visual cortex. J Neurosci 9:2432–2442.

Gittleman JL. 1986. Carnivore brain size, behavioral ecology, and phylogeny. J Mammal 67:23–26.

Globus A, Scheibel AB. 1967. Pattern and field in cortical structure: the rabbit. J Comp Neurol 1331:155–172.

Goodrich JM, Miquelle DG, Smirnov EN, Kerley LL, Quigley HB, Hornocker MG. 2010. Spatial structure of Amur (Siberian) tigers (*Panthera tigris altaica*) on Sikhote-Alin Biosphere Zapovednik, Russia. J Mammal 91:737–748.

Groos WP, Ewing LK, Carter CM, Coulter JD. 1978. Organization of corticospinal neurons in the cat. Brain Res 143: 393–419.

Hassler R, Muhs-Clement K. 1964. Architektonischer Aufbau des sensomotorischen und parietalen Cortex der Katze. J Hirnforsch 6:377–420.

Hastie T, Tibshirani R, Friedman J. 2009. The elements of statistical learning, 2nd ed. New York: Springer.

Hayes TL, Lewis DA. 1995. Anatomical specialization of the anterior motor speech area: hemispheric differences in magnopyramidal neurons. Brain Lang 49:289–308.

Hemmer H. 1968. Untersuchungen zur Stammesgeschichte der Pantherkatzen (Pantherinae). Teil II. Sudien zur Ethologie des *Neofelis nebulosa* (Griffith 1821) und des Irbis *Uncia uncia* (Schreber 1775). Veröff Zool Staatssamml München 12:155–247.

Higo, S, Udaka N, Tamamaki N. 2007. Long-range GABAergic projection neurons in the cat neocortex. J Comp Neurol 503:421–431.

Hof PR, Sherwood CC. 2005. Morphomolecular neuronal phenotypes in the neocortex reflect phylogenetic relationships among certain mammalian orders. Anat Rec 287: 1153–1163.

Hof PR, Van der Gucht E. 2007. Structure of the cerebral cortex of the humpback whale, *Megaptera novaeangliae* (Cetacea, Mysticeti, Balaenopteridae). Anat Rec 290: 1–31.

Hof PR, Nimchinsky EA, Young WG, Morrison JH. 2000. Numbers of Meynert and layer IVB cells in area V1: a stereologic analysis in young and aged macaque monkeys. J Comp Neurol 420:113–126.

Horner CH, Arbuthnott E. 1991. Methods of estimation of spine density—are spines evenly distributed throughout the dendritic field? J Anat 177:179–184.

Hubel DH, Wiesel TN. 1959. Receptive fields of single neurons in the cat's striate cortex. J Physiol 148:574–591.

Hubel DH, Wiesel TN. 1962. Receptive fields, binocular interaction and functional architecture in the cat's visual cortex. J Physiol 160:106–154.

Hübener M, Schwarz C, Bolz J. 1990. Morphological types of projection neurons in layer 5 of cat visual cortex. J Comp Neurol 301:655–674.

Hutsler JJ, Lee D-G, Porter KK. 2005. Comparative analysis of cortical layering and supragranular layer enlargement in rodent carnivore and primate species. Brain Res 1052:71–81.

Innocenti GM, Vercelli A. 2010. Dendritic bundles, minicolumns, columns, and cortical output units. Front Neuroanat 4:11.

Innocenti GM, Manger PR, Masiello I, Colin I, Tettoni L. 2002. Architecture and callosal connections of visual areas 17,18, 19 and 21 in the ferret (*Mustela putorius*). Cereb Cortex 12:411–422.

Jacobs B, Scheibel AB. 1993. A quantitative dendritic analysis of Wernicke's area in humans. I. Lifespan changes. J Comp Neurol 327:83–96.

Jacobs B, Scheibel AB. 2002. Regional dendritic variation in primate cortical pyramidal cells. In: Cortical areas: unity and diversity. (Conceptual advances in brain research series, Schüz A, Miller R, eds. London: Taylor & Francis, p 111–131.

Jacobs B, Driscoll L, Schall M. 1997. Life-span dendritic and spine changes in areas 10 and 18 of human cortex: a quantitative Golgi study. J Comp Neurol 386:661–680.

Jacobs B, Schall M, Prather M, Kapler E, Driscoll L, Baca S, Jacobs J, Ford K, Wainwright M, Treml M. 2001. Regional dendritic and spine variation in human cerebral cortex: a quantitative Golgi study. Cereb Cortex 11:558–571.

Jacobs B, Lubs J, Hannan M, Anderson K, Butti C, Sherwood CC, Hof PR, Manger PR. 2011. Neuronal morphology in the African elephant (*Loxodonta africana*) neocortex. Brain Struct Funct 215:273–298.

Jacobs B, Johnson NL, Wahl D, Schall M, Maseko BC, Lewandowski A, Raghanti MA, Wicinski B, Butti C, Hopkins WD, Bertelsen MF, Walsh T, Roberts JR, Reep RL, Hof PR, Sherwood CC, Manger PR. 2014. Comparative neuronal morphology of the cerebellar cortex in afrotherians, carnivores, cetartiodactyls, and primates. Front Neuroanat 8:24.

Jacobs B, Harland T, Kennedy D, Schall M, Wicinski B, Butti C, Hof PR, Sherwood CC, Manger PR. 2015a. The neocortex of cetartiodactyls. II. Neuronal morphology of the visual and motor cortices in the giraffe (*Giraffa camelopardalis*). Brain Struct Funct 220:2851–2872.

Jacobs B, Lee L, Schall M, Raghanti MA, Lewandowski A, Kottwitz JJ, Roberts JF, Hof PR, Sherwood CC. 2015b. Neocortical neuronal morphology in the newborn giraffe (*Giraffa camelopardalis tipelskirchi*) and African elephant (*Loxodonta africana*). J Comp Neurol 524:257–287.

Johnson WE, Eizirik E, Pecon-Slattery J, Murphy WJ, Antunes A, Teeling E, O'Brien SJ. 2006. The late Miocene radiation of modern Felidae: a genetic assessment. Science 311:73–77.

Kaas JH. 2000. Why is brain size so important: design problems and solutions as neocortex gets bigger or smaller. Biol Skrif 1:7–23.

Kaiserman-Abramof IR, Peters A. 1972. Some aspects of the morphology of Betz cells in the cerebral cortex of the cat. Brain Res 43:527–546.

Katz LC. 1987. Local circuitry of identified projection neurons in cat visual cortex brain slices. J Neurosci 7:1223–1249.

Kelly JP, van Essen DC. 1974. Cell structure and function in the visual cortex of the cat. J Physiol 238:515–547.

Kisvárday ZF, Gulyas A, Beroukas D, North JB, Chub IW, Somogyi P. 1990. Synapses, axonal and dendritic patterns of GABA-immunoreactive neurons in human cerebral cortex. Brain 113:793–812.

Kitchener AC, Beaumont MA, Richardson D. 2006. Geographical variation in the clouded leopard, *Neofelis nebulosa*, reveals two species. Curr Biol 16:2377–2383.

Lewis B. 1878. On the comparative structure of the cortex cerebri. Brain 1:79–86.

Lund JS, Henry GH, Macqueen CL, Harvey AR. 1979. Anatomical organization of the primary visual cortex (area 17) of the cat. A comparison with area 17 of the macaque monkey. J Comp Neurol 184:599–618.

Lund JS, Lewis DA. 1993. Local circuit neurons of the developing mature macaque prefrontal cortex: Golgi and immunocytochemical characteristics. J Comp Neurol 328:282–312.

Luo S-J, Kim J-H, Johnson WE, van der Walt J, Martenson J, Yuhki N, Miquelle DG, Uphyrkina O, Goodrich JM, Quigley HB, Tilson R, Brady G, Martelli P, Subramaniam V, McDougal C, Hean S, Huang S-Q, Pan W, Karanth UK, Sunquist M, Smith JLD, O'Brien SJ. 2004. Phylogeography and genetic ancestry of tigers (*Panthera tigris*). PLOS Biol 2:e442.

Manger PR, Cort J, Ebrahim N, Goodman A, Henning J, Karolia M, Rodrigues S-L, Strkalj G. 2008. Is 21st century neuroscience too focused on the rat/mouse model of brain function and dysfunction? Front Neuroanat 2:5.

Manger PR, Spocter MA, Patzke N. 2013. The evolutions of large brain size in mammals: the 'over-700-gram club quartet.' Brain Behav Evol 82:68–78.

Marin-Padilla M. 1992. Ontogenesis of the pyramidal cell of the mammalian neocortex and developmental cytoarchitectonics: a unifying theory. J Comp Neurol 321: 223–240.

Matsubara JA, Chase R, Thejomayen M. 1996. Comparative morphology of three types of projection-identified pyramidal neurons in the superficial layers of cat visual cortex. J Comp Neurol 366:93–108.

Mazák V. 1981. *Panthera tigris*. Mammal Species 152:1–8.

Mellott JG, Van der Gucht E, Lee CC, Carrasco A, Winder JA, Lomber SG. 2010. Areas of cat auditory cortex as defined by neurofilament proteins expressing SMI-32. Hear Res 267:119–136.

Mendizabal-Zubiaga JL, Reblet C, Bueno-López JL. 2007. The underside of the cerebral cortex: layer V/VI spiny inverted neurons. J Anat 211:223–236.

Meyer G. 1987. Forms and spatial arrangement of neurons in the primary motor cortex of man. J Comp Neurol 262: 402–428.

Meynert T. 1867. Der Bau der Gross-Hirnrinde und seiner örtlichen Verschiedenheiten, nebst einen pathologisch-anatomisch Corollarium. Vierteljahrsschr Psychiatr 1(77–93):125–217.

Mitani A, Shimokouchi M, Itoh K, Nomura S, Kudo M, Mizuno N. 1985. Morphology and laminar organization of electrophysiologically identified neurons in primary auditory cortex in the cat. J Comp Neurol 235: 430–447.

Morest DK, Morest RR. 1966. Perfusion-fixation of the brain with chrome-osmium solutions for the rapid Golgi method. Am J Anat 118:811–831.

Mountcastle VB. 1997. The columnar organization of the neocortex. Brain 120:701–722.

Nowell K, Jackson P. 1996. Wild cats. Gland, Switzerland: International Union for Conservation of Nature.

O'Leary JL. 1941. Structure of the area striata of the cat. J Comp Neurol 75:131–164.

Peters A, Kara DA. 1985. The neuronal composition of area 17 of rat visual cortex. I. The pyramidal cells. J Comp Neurol 234:218–241.
Peters A, Kara DA. 1987. The neuronal composition of area 17 of rat visual cortex. IV. The organization of pyramidal cells. J Comp Neurol 260:573–590.
Peters A, Regidor J. 1981. A reassessment of the forms of nonpyramidal neurons in area 17 of cat visual cortex. J Comp Neurol 203:685–716.
Peters A, Yilmaz E. 1993. Neuronal organization in area 17 of cat visual cortex. Cereb Cortex 3:49–68.
Phillips CG. 1956. Intracellular records from Betz cells in the cat. Q J Physiol Cogn Med Sci 41:58–69.
Povysheva NV, Zaitsev AV, Kröner S, Krimer OA, Rotaru DC, González-Burgos G, Lewis DA, Krimer LS. 2007. Electrophysiological differences between neurogliaform cells from monkey and rat prefrontal cortex. J Neurophysiol 97:1030–1039.
Preuss TM. 1995. Do rats have a prefrontal cortex? The Rose-Woolsey-Akert program reconsidered. J Cogn Neurosci 7: 1–24.
Qi H-X, Jain N, Preuss TM, Kaas JH. 1999. Inverted pyramidal neurons in chimpanzee sensorimotor cortex are revealed by immunostaining with monoclonal antibody SMI-32. Somatosens Mot Res 16:49–56.
Rockland KS, Ichinohe N. 2004. Some thoughts on cortical minicolumns. Exp Brain Res 158:265–277.
Ramón y Cajal S. 1911. Histologie du système nerveux de l'homme et des vertébrés. Vol 2. Trans. by Azoulay L. Paris: Maloine.
Ramon-Moliner E. 1961a. The histology of the postcruciate gyrus in the cat. I. Quantitative studies. J Comp Neurol 117:43–62.
Ramon-Moliner E. 1961b. The histology of the postcruciate gyrus in the cat. II. A statistical analysis of the dendritic distribution. J Comp Neurol 117:63–76.
Ramon-Moliner E. 1961c. The histology of the postcruciate gyrus in the cat. III. Further observations. J Comp Neurol 117:229–249.
Reep RL, Johnson JI, Switzer RC, Welker WI. 1989. Manatee cerebral cortex: cytoarchitecture of the frontal region in *Trichechus manatus latirostris*. Brain Behav Evol 34:365–386.
Rioch DM. 1937. A physiological and histological study of the frontal cortex of the seal (*Phoca vitulina*). Biol Bull 73: 591–602.
Rivara C-B, Sherwood CC, Bouras C, Hof PR. 2003. Stereologic characterization and spatial distribution patterns of Betz cells in the human primary motor cortex. Anat Rec 270:137–151.
Sanides F, Sanides D. 1972. The "extraverted neurons" of the mammalian cerebral cortex. Z Anat Entwickl Gesch 136: 272–293.
Sasaki S, Iwata M. 2001. Ultrastructural study of Betz cells in the primary motor cortex of the human brain. J Anat 199:699–708.
Scannell JW, Blakemore C, Young MP. 1995. Analysis of connectivity in the cat cerebral cortex. J Neurosci 15:1463–1483.
Schadé, JP, Caveness WF. 1968. IV. Alteration in dendritic organization. Brain Res 7:59–86.
Scheibel ME, Scheibel AB. 1978a. The dendritic structure of the human Betz cell. In: Brazier MAB, Petsche H, editors. Architectonics of the cerebral cortex. IBRO monographic series. Vol. 3. New York: Raven Press. p 43–57.
Scheibel ME, Scheibel AB. 1978b. The methods of Golgi. In: Robertson RT, editor. Neuroanatomical research techniques. New York: Academic Press. p 89–114.
Sherwood CC, Lee PW, Rivara CB, Holloway RL, Gilissen EP, Simmons RM, Hakeem A, Allman JM, Erwin JM, Hof PR. 2003. Evolution of specialized pyramidal neurons in primate visual and motor cortex. Brain Behav Evol 61:28–44.
Sherwood CC, Stimpson CD, Butti C, Bonar CJ, Newton AL, Allman JM, Hof PR. 2009. Neocortical neuron types in Xenarthra and Afrotheria: implications for brain evolution in mammals. Brain Struct Funct 213:301–328.
Sholl DA. 1953. Dendritic organization in the neurons of the visual and motor cortices of the cat. J Anat 87:387–406.
Simon A, Olah S, Molnar G, Szabadics J, Tamas G. 2005. Gap-junctional coupling between neurogliaform cells and various interneuron types in the neocortex. J Neurosci 25: 6278–6285.
Somogyi P, Kisvárday ZF, Martin KAC, Whitteridge D. 1983. Synaptic connections of morphologically characterized large basket cells in the striate cortex of cat. Neuroscience 10:261–294.
Steger R, Ramos RL, Cao R, Yang Q, Chen C-C, Dominici J, Brumberg JC. 2013. Physiology and morphology of inverted pyramidal neurons in the rodent neocortex. Neuroscience 248:165–179.
Sun HY, Lu XD, Tian JL, Cheng ST, Li DF, Dong HY. 2005. The wild population monitor of Amur tiger in Heilongjiang province. Forest Sci Technol 30:33–35.
Thomson AM, Bannister AP. 2003. Interlaminar connections in the neocortex. Cereb Cortex 13:5–14.
Thomson AM, West CD, Wang Y, Bannister AP. 2002. Synaptic connections and small circuits involving excitatory and inhibitory neurons in layers 2–5 of adult rat and cat neocortex: triple intracellular recordings and biocytin labeling in vitro. Cereb Cortex 12:936–953.
Uylings HBM, Ruiz-Marcos A, van Pelt J. 1986. The metric analysis of three-dimensional dendritic tree patterns: a methodological review. J Neurosci Methods 18:127–151.
Uylings HBM, Groenewegen HJ, Kolb B. 2003. Do rats have a prefrontal cortex? Behav Brain Res 146:3–17.
Valverde F. 1986. Intrinsic neocortical organization: some comparative aspects. Neuroscience 18:1–23.
Valverde F, Facal-Valverde MV. 1986. Neocortical layers I and II of the hedgehog (*Erinaceus europaeus*). Anat Embryol 173:413–430.
Van der Gucht E, Clerens S, Jacobs S, Arckens L. 2005. Light-induced Fos expression in phosphate-activated glutaminase- and neurofilament protein-immunoreactive neurons in cat primary visual cortex. Brain Res 1035: 60–66.
Van der Loos H. 1965. The "improperly" oriented pyramidal cell in the cerebral cortex and its possible bearing on problems of neuronal growth and cell orientation. Bull Johns Hopkins Hosp 117:228–250.
Van Brederode JFM, Foehring RC, Spain WJ. 2000. Morphological and electrophysiological properties of atypically oriented layer 2 pyramidal cells of the juvenile rat neocortex. Neuroscience 101:851–861.
Vercelli A, Innocenti GM. 1993. Morphology of visual callosal neurons with different locations, contralateral targets or patterns of development. Exp Brain Res 94:393–404.
Williams RS, Ferrante RJ, Caviness VS Jr. 1978. The Golgi rapid method in clinical neuropathology: the morphologic consequences of suboptimal fixation. J Neuropathol Exp Neurol 37:13–33.
Wilting A, Buckley-Beason VA, Feldhaar H, Gadau J, O'Brien SJ, Linsenmair KE. 2007. Clouded leopard phylogeny revisited: support for species recognition and population division between Borneo and Sumatra. Front Zool 4:15.
Winer JA. 1984a. Anatomy of layer IV of cat primary auditory cortex (AI). J Comp Neurol 224:535–567.

Winer JA. 1984b. The non-pyramidal neurons in layer III of cat primary auditory cortex (AI). J Comp Neurol 229: 512–530.
Winer JA. 1984c. The pyramidal neurons in layer III of cat primary auditory cortex (AI). J Comp Neurol 229: 476–496.
Winer JA. 1985. Structure of layer II in cat primary auditory cortex (AI). J Comp Neurol 238:10–37.
Winer JA, Prieto JJ. 2001. Layer V in cat primary auditory cortex (AI): cellular architecture and identification of projection neurons. J Comp Neurol 434:379–412.
Wittenberg GM, Wang SS-H. 2008. Evolution and scaling of dendrites. In: Stuart G, Spruston N, Hausser N, editors. Dendrites. New York: Oxford University Press, New York. p 43–67.
Yamamoto T, Samejima A, Oka H. 1987. Morphologial features of layer V pyramidal neurons in the cat parietal cortex: an intracellular HRP study. J Comp Neurol 265:380–390.
Yu L, Zhang Y. 2005. Phylogenetic studies of pantherine cats (Felidae) based on multiple genes, with novel application of nuclear-fibrinogen intron 7 to carnivores. Mol Phylogenet Evol 35:483–495.
Zsiros V, Maccaferri G. 2005. Electrical coupling between interneurons with different excitable properties in the stratum lacunosum-moleculare of the juvenile CA1 rat hippocampus. J Neurosci 25:8686–8695.